

AD-A160 146

## PROBABILISTIC EVALUATION OF INDIVIDUAL AIRCRAFT

142

TRACKING TECHNIQUES(U) AIR FORCE INST OF TECH

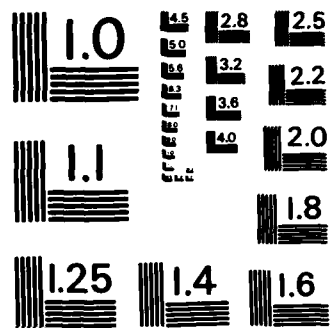
WRIGHT-PATTERSON AFB OH SCHOOL OF SYST.. R L WILKINSON

UNCLASSIFIED

SEP 85 AFIT/GSM/ENS/855-32

F/G 1/3

NL



MICROCOPY RESOLUTION TEST CHART  
NATIONAL BUREAU OF STANDARDS-1963-A

AD-A160 146

2



PROBABILISTIC EVALUATION OF  
INDIVIDUAL AIRCRAFT TRACKING TECHNIQUES

THESIS

Rodney L. Wilkinson  
Captain, USAF

AFIT/GSM/ENS/85S-32

DTIC FILE COPY

DTIC  
ELECTE  
OCT 09 1985  
S D E

DEPARTMENT OF THE AIR FORCE  
AIR UNIVERSITY  
**AIR FORCE INSTITUTE OF TECHNOLOGY**

Wright-Patterson Air Force Base, Ohio

This document has been approved  
for public release and sale; its  
distribution is unlimited.

85 10 8 082

AFIT/GSM/ENS/85

PROBABILISTIC EVALUATION OF  
INDIVIDUAL AIRCRAFT TRACKING TECHNIQUES

THESIS

Rodney L. Wilkinson  
Captain, USAF

AFIT/GSM/ENS/85S-32

DTIC  
SELECTE  
001 0 9 1985  
S D  
E

Approved for public release; distribution unlimited

The contents of the document are technically accurate, and no sensitive items, detrimental ideas, or deleterious information are contained therein. Furthermore, the views expressed in the document are those of the author(s) and do not necessarily reflect the views of the School of Systems and Logistics, the Air University, the United States Air Force, or the Department of Defense.

<b>Accession For</b>	
NTIS GRA&I	<input checked="checked" type="checkbox"/>
DTIC TAB	<input type="checkbox"/>
Unannounced	<input type="checkbox"/>
Justification	
By _____	
Distribution/	
Availability Codes	
Avail and/or	
Dist	Special
<b>A-1</b>	



**PROBABILISTIC EVALUATION OF  
INDIVIDUAL AIRCRAFT TRACKING TECHNIQUES**

**THESIS**

**Presented to the Faculty of  
the School of Systems and Logistics  
of the Air Force Institute of Technology  
Air University  
In Partial Fulfillment of the  
Requirements for the Degree of  
Master of Science in Systems Management**

**Rodney L. Wilkinson, B.S.  
Captain, USAF**

**September 1985**

**Approved for public release; distribution unlimited**

## Acknowledgements

This thesis was written with the support and encouragement of the Flight Dynamics Laboratory (AFWAL/FIBEC) at Wright-Patterson Air Force Base. I would like to express my special thanks to Mr. Robert M. Engle who served as technical consultant and mentor throughout the effort.

My advisor was LTC Joseph Coleman (AFIT/ENS), who managed somehow to keep me "in scope" despite my tendency to expand the topic. Ms. Marge Artley (AFWAL/FIBEC) offered many helpful comments and opinions which greatly enhanced the quality of this report. Dr. Tom Christian (Warner-Robins Air Logistics Center) and Mr. Phil Allen (Ogden Air Logistics Center) provided valuable information on the IAT program. Dr. Jack Lincoln, Mr. Harold Howard, Mr. Ed Davidson, and Mr. Dave Erskine (ASD/ENFS) were most helpful in defining the problem and keeping the scenario realistic. If the technique proposed in this thesis succeeds, it is due to the help of all of these people.

Finally, I would like to acknowledge the help of Lt Pat Alsup and Mr. Clare Paul (AFWAL/FIBEC), and of Mr. Joel Rice (AFIT/ADO Consultant). Each of them donated several hours to assist me with some portion of the work. To my wife Yvonne, I express a special thanks for her patience and understanding.

Rodney L. Wilkinson

## Table of Contents

	Page
Acknowledgements .....	ii
List of Figures .....	v
List of Tables .....	vii
Abstract .....	x
I. Introduction .....	1
Problem Statement .....	3
General Issue .....	3
Specific Problem .....	4
Research Question .....	4
Scope and Limitations .....	5
The Aircraft Structure .....	5
The Flight Environment .....	6
The Recording Device .....	6
Nomenclature .....	7
Outline of Report .....	9
II. Background: The USAF Individual Aircraft Tracking Program .....	10
Evolution of the IAT Program .....	10
The Current IAT Program .....	13
Data Collection .....	15
Analysis .....	15
Application of Results .....	16
Summary .....	17
III. Methodology .....	18
Scenario .....	18
The Aircraft .....	18
The Load History .....	18
The IAT Device .....	20
Life Prediction Model .....	24
Simulation Procedure .....	24
Assumptions .....	26
Data Capture Rate .....	27
Initial Flaw Size .....	28
Variables .....	28
Material Properties .....	28
Load Histories .....	34
Stress Levels .....	36

	Page
The Simulation .....	36
Summary .....	38
IV. Results .....	39
Simulation Output Data .....	41
Analysis of Output Data .....	50
Determining Distributions .....	50
Structural Lives .....	62
Inspection Crack Lengths .....	65
Summary of Results .....	68
V. Discussion .....	70
Material Properties .....	70
Load History Variations .....	73
Stress Levels .....	76
Combined Effects .....	76
Summary .....	80
VI. Conclusions and Recommendations .....	81
Conclusions .....	81
Recommendations .....	83
Appendix A: Material Properties Simulation .....	85
Appendix B: CRACKS4: A Life Prediction Model .....	115
Appendix C: A Formula for Structural Life? .....	123
Bibliography .....	128
Vita .....	131

## List of Figures

Figure	Page
1. Structural Geometry .....	19
2. Exceedance Curve for Baseline Load History .....	21
3. Determination of an Inspection Interval .....	25
4. Stochastic Approach to Inspection Intervals .....	26
5. Crack Growth Curves (68 Curves, 11,152 Points) ..	30
6. Crack Growth Rate Curves (Linear Range Only) ....	32
7. Exceedance Curve for Baseline Load History .....	35
8. Baseline Curve Representing Expected Crack Growth Behavior .....	40
9. Histogram for Structural Lives at 38 ksi .....	50
10. Histogram for Inspection Crack Lengths at 38 ksi.	50
11. Histogram for Structural Lives at 40 ksi .....	51
12. Histogram for Inspection Crack Lengths at 40 ksi.	51
13. Histogram for Structural Lives at 42 ksi .....	52
14. Histogram for Inspection Crack Lengths at 42 ksi.	52
15. Histogram for Overall Distribution of Structural Lives .....	59
16. Histogram for Overall Distribution of Inspection Crack Lengths .....	59
17. Schematic of a Stochastic Crack Growth Curve ....	61
A1. Crack Growth Rate Curves (68 Curves, 8228 Points)	87
A2. Histogram for Walker Slope N .....	92
A3. Histogram for Walker Intercept C .....	92
A4. Histogram for $\ln(C)$ .....	95
A5. Probability Density Functions Overlayed on Histogram for N .....	97

Figure	Page
A6. Simulation Program Listing .....	105
A7. Histogram for Measured Lives .....	112
A8. Histogram for Lives Obtained by Regression .....	113
A9. Histogram for Lives Simulated Based on a Normal Distribution for N .....	113
A10. Histogram for Lives Simulated Based on a Weibull Distribution for N .....	114
B1. Schematic of CRACKS4 Inputs .....	117
B2. Sample Output from CRACKS4 Program .....	118

## List of Tables

Table	Page
1. Selected Load Histories .....	22
2. Exceedances for Each Load History Variation .....	23
3. Random Variable Inputs to the Simulation .....	38
4. Summary of Simulation Results by Stress Level ...	42
5. Aircraft Lives in Flight Hours, Based on a Stress of 38 ksi .....	43
6. Aircraft Lives in Flight Hours, Based on a Stress of 40 ksi .....	44
7. Aircraft Lives in Flight Hours, Based on a Stress of 42 ksi .....	45
8. Crack Length (inches) at 2350 Hour Depot-Level Inspection, Based on a Maximum Stress of 38 ksi .	46
9. Crack Length (inches) at 2350 Hour Depot-Level Inspection, Based on a Maximum Stress of 40 ksi .	47
10. Crack Length (inches) at 2350 Hour Depot-Level Inspection, Based on a Maximum Stress of 42 ksi .	48
11. Chi-squared fit for Normal Distribution of Lives at a Maximum Stress of 38 ksi .....	54
12. Chi-squared fit for Normal Distribution of Lives at a Maximum Stress of 40 ksi .....	55
13. Chi-squared fit for Normal Distribution of Lives at a Maximum Stress of 42 ksi .....	55
14. Chi-squared fit for Normal Distribution of Ln(Crack Length) at a Maximum Stress of 38 ksi ..	56
15. Chi-squared fit for Normal Distribution of Ln(Crack Length) at a Maximum Stress of 38 ksi ..	56
16. Chi-squared fit for Normal Distribution of Ln(Crack Length) at a Maximum Stress of 38 ksi ..	57
17. Chi-squared fit for Normal Distribution of Lives -- All Tests .....	60

Table	Page
18. Chi-squared fit for Normal Distribution of Ln(Crack Length) -- All Tests .....	60
19. Probabilities Associated with the Standard Normal Distribution .....	63
20. Probability of Structural Failure .....	64
21. Required Inspection Intervals .....	65
22. Probability of Undetectable Crack Sizes .....	68
23. Summary of Simulation Results by Material Constants .....	71
24. Groups of Material Constants that Produced Statistically Similar Structural Lives .....	72
25. Groups of Material Constants that Produced Statistically Similar Inspection Crack Lengths ..	72
26. Summary of Simulation Results by Load History ...	74
27. Summary of Simulation Results by Stress Level ...	77
28. Comparison of Simulated and Predicted Lives .....	79
A1. Summary of Curve-Fit Results .....	89
A2. Curve-Fit Results .....	90
A3. Chi-squared fit for Weibull Distribution of N ...	94
A4. Chi-squared fit for Normal Distribution of Ln(C). ..	95
A5. Chi-squared fit for Normal Distribution of N ....	96
A6. Runs Above and Below the Mean Test for Independence .....	98
A7. Chi-squared Test for Uniformity -- Observed Values .....	99
A8. Chi-squared Test for Uniformity -- Chi-squared Statistic .....	99
A9. Test for Equality of Means and Variances -- Normal Variates .....	110
A10. Test for Equality of Means and Variances -- Weibull Variates .....	110

Table	Page
A11. Chi-squared fit for Normal Distribution of Ln(Life) .....	111
C1. Root-mean-square Factors for Load Histories .....	124
C2. Selected Parameters for Baseline Load History ...	126

## Abstract

A study was conducted in order to demonstrate a technique for comparing the outputs of various individual aircraft tracking (IAT) systems. There were two objectives: (1) to determine the distribution of structural lives that could be expected based on a single IAT scenario, and (2) to evaluate the feasibility of replacing the current universal IAT safety factor with specific statistical calculations that consider the strengths and weaknesses of each IAT system. The ultimate goal of this thesis was to begin the transition of individual aircraft tracking from a deterministic approach to a stochastic one.

A simulation was performed which included twelve aircraft, each flying five different load history variations at three gross weights. Initial structural damage was assumed based on a "reset" flaw size after nondestructive inspection. Structural lives were normally distributed with a mean of approximately 4700 flight hours. The cracks present at the one-half lifetime depot inspection were lognormally distributed. Using these distributions, the probabilities of structural failure were calculated for several inspection intervals. Repeating this process for other IAT scenarios would allow a direct comparison of various IAT systems. Eventually, such a process could lead to individual system safety factors, rather than the current universal safety factor.

# PROBABILISTIC EVALUATION OF INDIVIDUAL AIRCRAFT TRACKING TECHNIQUES

## I. Introduction

This thesis is intended to be the first in a series of programs designed to statistically evaluate the quality of output information from individual aircraft tracking (IAT) systems. By comparing the variability introduced by differences in structural materials, data collection methods, and analytical techniques, the strengths and weaknesses of each IAT system can be determined. Finally, through a series of trade-off and sensitivity studies, the most effective and efficient combination of parameters can be identified and incorporated into the "optimal" IAT system. The ultimate goal of these programs is to transition IAT from the current deterministic process to a stochastic approach. Thus, the current safety factor could be replaced by a statistical probability and confidence that the structure is in need of repair. An understanding of the effects of parameter variations on IAT structural life predictions is essential for this transition.

Before the length of a potential structural crack can be estimated, several factors must be known or assumed. First, the results of nondestructive inspections provide a 90 percent probability (with 95 percent confidence) that no cracks longer than some minimum detectable size are present.

That minimum detectable size becomes the assumed initial flaw size. Realistically, a crack exceeding the detectable size could be missed during inspection. On the other hand, few aircraft in the fleet actually have a crack of significant size at the most critical location, so the assumption of initial flaw size is conservative.

Once the flaw size is known or assumed, there are two more unknowns that make analysis difficult. The aircraft structural material (in this case, 2024-T3 aluminum) is not homogeneous. Different pieces of "identical" material behave differently under exactly the same loading conditions. In addition, no two structures ever encounter the same sequence of flight loads. Air Force programs such as the Loads/Environment Spectra Survey (4: Sec 2,9) and the IAT program collect data which helps to estimate structural loads, but the actual load history is never known. Thus, the inherent variability in material response, and the accuracy of our data collection and analysis of structural loads play a major role in the effectiveness of the IAT program.

The current deterministic IAT program depends on average or conservative values for the input variables discussed above. (A conservative value is one which may introduce error, but will always err to a safe direction. The most common use of conservative analysis is a "worst case" scenario.) If the underlying distributions for the

above parameters were known, a stochastic approach to IAT could replace the current deterministic program. Average case and worst case analysis would then give way to confidence intervals and probability estimates. Until then, stochastic techniques offer improvements in another way. By varying the parameters for which we do understand underlying probabilities, various IAT systems could be compared directly to one another, and the universal IAT safety factor could be replaced by more realistic individual system safety factors.

The objective just discussed is obviously beyond the scope of a thesis. However, the principles and techniques do not vary significantly with the magnitude of the simulation. Therefore, the focus of this thesis will be on demonstrating a feasible approach for comparing the various IAT systems, rather than on obtaining a complete solution to the problem as discussed.

### Problem Statement

General Issue. Can the statistical concepts of probability and confidence be applied to individual aircraft tracking system parameters to determine the quality of IAT system outputs?

Currently, inspection intervals for USAF aircraft are arbitrarily based on one half of the interval calculated using IAT methods. Such a "safety factor" is used because of: (1) the possibility that an existing structural crack

was not detected during the last inspection, and (2) a lack of confidence in the output information provided by IAT. Since IAT systems use deterministic inputs and techniques to predict stochastic processes, the safety factor is justified. However, the more efficient approach would be to model the stochastic processes themselves.

**Specific Problem.** Can the arbitrary safety factor currently used for all IAT systems be replaced by specific statistical calculations which consider the strengths and weaknesses of each system?

In order to replace the IAT safety factor, stochastic IAT techniques must provide a reasonable estimate of structural life (as compared to current methods), based on a predetermined level of significance. Current deterministic analyses rely on average or approximated values for input parameters such as aircraft gross weight and material properties, and compensate for the resulting error by applying a safety factor. The proposed stochastic approach uses randomly selected values for all significant input parameters, based on their underlying probability distributions. The stochastic inspection interval is then determined by a lower-tailed hypothesis test on the resulting distribution of probable structural lives.

**Research Question.** For a selected stochastic IAT scenario, what is the distribution of probable structural lives?

### Scope and Limitations

The intent of this study is not to immediately replace the IAT safety factor with a statistical formula. Instead, a technique is proposed by which the strengths and weaknesses of various IAT systems can be compared directly to one another. Using this technique, IAT systems can be evaluated and ranked based on output quality (accuracy and precision), and the safety factor can be adjusted to reflect the true uncertainty associated with each IAT system.

Many parameters affect the accuracy and precision of output information provided by individual aircraft tracking systems. The parameters fall into three broad categories according to the source of variability: (1) the aircraft structure, (2) the flight environment, and (3) the recording device. The quality of current data analysis techniques was not considered per se. However, the success of any IAT analysis depends heavily on the reconstruction of the original flight environment from recording device output, as well as an accurate representation of structural material properties.

The Aircraft Structure. For simplicity, the "structure" was defined as the location of highest critical stress near the wing root of a front-line NATO fighter aircraft. The relationship between normal accelerations (g forces) and stress level was calculated based on a linear decline in gross weight from take-off to landing.

Variability in material properties was limited to that expected for a single production batch of 2024-T3 aluminum alloy (29), since a representative fleet-wide mix of material properties was not available. Only crack growth rate parameters were varied. Tensile yield and ultimate strengths and material fracture toughness were held constant. In addition, the size of the largest initial structural crack present at the critical location was assumed to be one-eighth inch throughout the simulation.

The Flight Environment. The real test of an IAT system is how well its output corresponds to the actual flight environment. Therefore, the aircraft flight load history was treated as realistically as possible. The only limitation of any consequence was that compressive loads were clipped at zero. For each load history variation, aircraft gross weights were calculated as follows: Aircraft gross weight variations were assumed to be normally distributed with a standard deviation of five percent of the mean. Because of resource limitations, the three values chosen to represent gross weight were the mean value, one standard deviation below the mean, and one standard deviation above the mean.

The Recording Device. The IAT recorder simulated in this study collected 100 percent of the flight data available. Realistically, some of the data would be lost due to

malfunctions and system limitations (1). The effects of data capture rate should be considered in future simulations.

### Nomenclature

The terms, abbreviations, and acronyms used commonly throughout the thesis are explained below.

<u>Term or Symbol</u>	<u>Definition</u>
a	Half crack length measured from the hole edge to the crack tip
$a_{crit}$	Critical crack length which is sufficient to cause failure
$a_{NDE}$	The size of the smallest crack that can be reliably found by nondestructive evaluation (NDE)
ASIP	The Aircraft Structural Integrity Program
C	Constant used in the Walker equation to represent the intercept of the crack growth rate curve
Cycle	The load variation from valley to peak to valley load
$da/dn$	Crack growth rate
Data Capture Rate	The percentage of available data actually recorded by an IAT device and useful for analysis
Exceedance Curve	A cumulative frequency diagram representing the the occurrences of loading parameters such as the peak load of a particular load history
Flight	In this thesis, one hour of recorded structural loads data
g	The force equivalent to the standard pull of gravity. Usually derived from the load factor, $N_z$

<u>Term or Symbol</u>	<u>Definition</u>
IAT	Individual Aircraft Tracking
$\Delta K$	The stress intensity factor range used to express structural loading and geometry through a common factor so that dissimilar conditions can be compared
ksi	1000 pounds per square inch
Life	In this thesis, the remaining number of flight hours until structural failure, based on an assumed level of structural damage
$\ln(x)$	The natural logarithm of x
Load History	A sequence of flight loads which is repeated throughout the simulated life of an aircraft
m	A constant used in the Walker equation to account for the the effects of differing stress ratios on crack growth behavior
n	Number of load cycles
N	Constant used in the Walker equation to represent the slope of the crack growth rate curve
$N_z$	The load factor representing a magnification of structural loads due to maneuvering
Paris Equation	A power law relating crack growth rate to stress intensity factor
Peak	The highest load within a cycle
$r^2$	Coefficient of determination for a least squares regression fit
R	The stress ratio, or algebraic ratio of valley to peak load
$\sigma$	Stress Level

<u>Term or Symbol</u>	<u>Definition</u>
Safe Life	The number of remaining flight hours before undue risk of structural failure
Spectrum	A complete sequence of aircraft flight loads, comprised of one or more repetitions of the load history
Valley	The lowest load within a cycle
w	Width of a structural panel
Walker Equation	A power law which expresses crack growth rate as a function of stress intensity factor and stress ratio

### Outline of Report

This thesis is presented in five major sections. Chapter I outlines reasons for the study and its major goals. Chapter II gives a general overview of individual aircraft tracking and the Aircraft Structural Integrity Program. The methods used to conduct the simulation are described in Chapter III, along with the scenario assumed for the aircraft and flight conditions. Results of the study are presented in Chapter IV. Finally, Chapter V discusses the impact of various input parameters on simulation output.

Conclusions and recommendations are listed in Chapter VI. Three appendices provide detailed information for the interested reader.

## II. Background:

### The USAF Individual Aircraft Tracking Program

Individual aircraft tracking is the primary tool used by the Air Force to schedule inspections, maintenance, and repairs for operational aircraft (4: Sec 2,11). IAT is often referred to as "tail number" tracking because the program monitors the usage of every airplane in the USAF inventory and provides a current estimate of each plane's structural condition (11). This chapter discusses the origins of the IAT program and provides a general overview of IAT tasks.

#### Evolution of the IAT Program

Until the 1950s, the Air Force used only static testing to verify proposed structural designs for new aircraft (22:3). Several crashes during the early 1950s, however, prompted scientists to warn that merely designing the structure to withstand a single maximum load was not enough. The crashes were caused by the initiation and growth of cracks resulting from the repeated occurrence of seemingly insignificant structural loads -- a process known as "fatigue" (22:9). The warnings were not heeded. Keeping simple design guidelines with appropriate "safety factors" appeared much more economically attractive than changing to the proposed fatigue evaluation program.

Opinions changed rapidly in 1958. During the five week period from 13 March to 15 April, five B-47 bombers crashed

due to structural failures (22:11). The B-47 was the United States' front-line medium range bomber, and the crashes received high level attention. Four of the five accidents were traced directly to fatigue problems (22:13). After the panic to keep the B-47 fleet from being grounded subsided, General Curtis LeMay, Air Force Vice Chief of Staff, wasted no time in taking action. On 12 June 1958, he approved the "Aircraft Structural Integrity" program (22:20).

The primary objectives of this program were (a) to control structural fatigue in the operational aircraft fleet, (b) to devise methods of accurately predicting aircraft service life, and (c) to provide the design know-how and test techniques required to avoid structural and sonic fatigue problems in future weapons systems. (22:20)

The Aircraft Structural Integrity Program (ASIP) gained support, momentum, and funding. Within the next year, the static test required for new aircraft designs was supplemented with a mandatory fatigue certification test (22:26). Several documents defined and refined ASIP requirements throughout the 1960s. The most notable ones, ASD Technical Note 61-141 and ASD Technical Report 66-57, were developed within the Aeronautical Systems Division at Wright-Patterson Air Force Base (22:33-39). Unfortunately, none of the documents provided clear authority to implement ASIP requirements. A lot of excellent research yielded limited results because of industry's resistance to change and the government's lack of formal direction.

Finally, the Air Force published Regulation 80-13 in June 1969 (22:36). The regulation made compliance with ASIP requirements mandatory for all future USAF aircraft systems, and added a new requirement for the periodic inspection of operational aircraft (8). Inspection intervals were determined based on the results of fatigue certification tests and the average flying conditions for each fleet of aircraft. Since all aircraft were now inspected at carefully determined intervals, the chances of another catastrophe like the B-47 incidents seemed remote.

The Air Force rested comfortably for only six months. In December 1969, a new F-111A crashed in the Nevada desert after the fatigue failure of a wing pivot fitting (22:41; 27:169). During the same time frame, another new USAF aircraft known as the C-5 Galaxy began to develop severe problems with widespread structural cracking (11). Problems showed up in B-52, KC-135, and F-4 aircraft structures shortly thereafter (11). The resulting investigations throughout the Air Force and industry led to two startling conclusions: (1) No "perfect" aircraft structure existed. Small cracks and flaws resulting from the manufacturing process could be present in any structure. (2) Operational flying conditions seldom matched the conditions used for fatigue certification testing, and many structures failed well before the scheduled inspection time (11).

Solving the first problem was costly, but relatively straightforward. Aircraft designers were directed to assume that a given flaw size was present at each critical structural detail after manufacturing, and to account for the influence of that flaw in their analysis (26:135). The second problem required that aircraft inspection intervals be revised. Since flaws could be present in any structure, and since operational flying invariably differed from anticipated usage, each aircraft had to be considered individually (4: Sec 2,1). Implementing the procedures necessary for the tracking of individual airplanes was difficult, but the task showed steady progress (22:43,44).

Military Standard 1530 formalized one of the Air Force's new ASIP requirements in September 1972. The design technique using assumed structural flaws was named Damage Tolerance. The new Individual Aircraft Tracking Program was officially born in December 1975 when Military Standard 1530 was updated and named 1530A. By 1976, AF Regulation 80-13 was totally rewritten, and a host of associated standards and specifications were added to further define and clarify ASIP requirements (22:23). The Air Force did not intend to face catastrophes like the B-47 and F-111 incidents again.

#### The Current IAT Program

The objective of individual aircraft tracking is "to monitor the usage of each individual airplane and to provide

structural inspection and maintenance schedules based on predicted flaw growth" (4: Sec 2,11). Thus for each airplane, the IAT program monitors the size of predicted structural flaws (cracks), the number of hours flown each month, and the severity of recorded flight loads. The time calculated for the cracks to reach the largest "safe" crack size under the monitored conditions determines the scheduled inspection interval.

Data obtained from IAT systems are also used in several other ways (25:2). AF Logistics Command uses the information to establish maintenance requirements and schedule repairs. AF Systems Command continually updates design, test, and analysis requirements based on IAT data. The using command, who flies the airplanes, uses the data to determine when to rotate specific airplanes from one base to another. The using command also relies on IAT data when deciding whether repairing an airplane is economical or if that airplane should be retired. Because of the importance and volume of IAT data, any system designed to collect it must be accurate, reliable, and efficient (16:88).

The concept behind the IAT program is relatively simple, and the payoffs greatly exceed program costs. A closer look at the program, however, reveals that the tasks required to implement IAT on a daily basis are awesome. The following paragraphs describe the three basic tasks associated with

all IAT systems: data collection, analysis, and application of results (17:13).

Data Collection. The ultimate purpose of any IAT system is to "determine, directly or indirectly, the [potential] crack length at critical structural locations" (7:39). No current system has the capability to measure crack length directly, so some combination of other parameters must be measured and used to estimate crack length. The parameters most commonly recorded are vertical and lateral accelerations (g forces), airspeed, control surface position, gross weight, number of landings, and flight hours (5). Most of these values change constantly and can be determined only for specific points in time.

Analysis. Once all necessary IAT data are collected, they must be converted into some useful form by analysis. The analysis phase is very costly due to extensive computer and manpower requirements. Therefore, the choice of an appropriate analytical method is extremely important.

Cycle-by-cycle techniques are the most accurate because they consider all loads the aircraft encountered in the sequence that the loads occurred. The data and resources required to run a cycle-by-cycle analysis are about ten times the requirements for other methods (4: Sec 5,124).

Exceedance curve analysis is used extensively for fighter and attack aircraft (1). Exceedance curves are generated by recording the number of times that designated

load levels are exceeded during a fixed number of flight hours (18). The effect of a particular exceedance curve on crack growth can be determined in advance and simply looked up when data comes in from the aircraft (4: Sec 5,125). One major problem with this method is that it does not record the sequence in which flight loads occur. Load sequence does affect crack growth rates, but the error introduced is offset by the simplicity and economy of the exceedance curve method.

Fleet managers for bomber and transport aircraft rely primarily on parametric analysis (17). Since the missions of large aircraft are generally routine and predictable in terms of flight loads, only flight parameters are used in the analysis. For example, each type of flight segment (take-off, cruise, air refueling, etc.) has known characteristics. The analyst needs to know only the aircraft gross weight, flight segment type, and duration of the flight segment to determine the appropriate increment of crack growth. Parametric analysis is slightly less accurate than the exceedance curve method, but is much easier to implement on large aircraft. The cost and complexity of the two methods are about the same. (4: Sec 5,124-125)

Application of Results. Output from IAT analyses is commonly expressed as a factor called the "Damage Index" (25:66). The damage index is the ratio of the time required for the present damage (crack) to develop, to the total time

predicted for the initial damage to grow to failure. Thus a typical damage index would be between 0.0 and 1.0.

### Summary

The Individual Aircraft Tracking Program was initiated as a result of several catastrophic airplane crashes during the 1950s and 1960s. It was preceded by the Aircraft Structural Integrity Program and became part of ASIP in 1972 when Military Standard 1530 was published. The specific objective of individual aircraft tracking is to schedule maintenance and inspections for each airplane in terms of that airplane's actual usage. The tasks required to implement IAT are awesome, but the program works very well. The three major IAT functions are data collection, analysis, and application of results.

Current IAT systems may seem rather crude considering the state of technology in the United States today. These systems, however, do their job well (20). The IAT program must work in the field, not just in a laboratory. Extensive data requirements and complex analysis techniques may not be supportable in the "real world." In addition, managers cannot make an intelligent decision if the information provided by IAT is in the wrong format. Converting the deluge of IAT information to a single number for decision-makers is actually a quite remarkable feat.

### III. Methodology

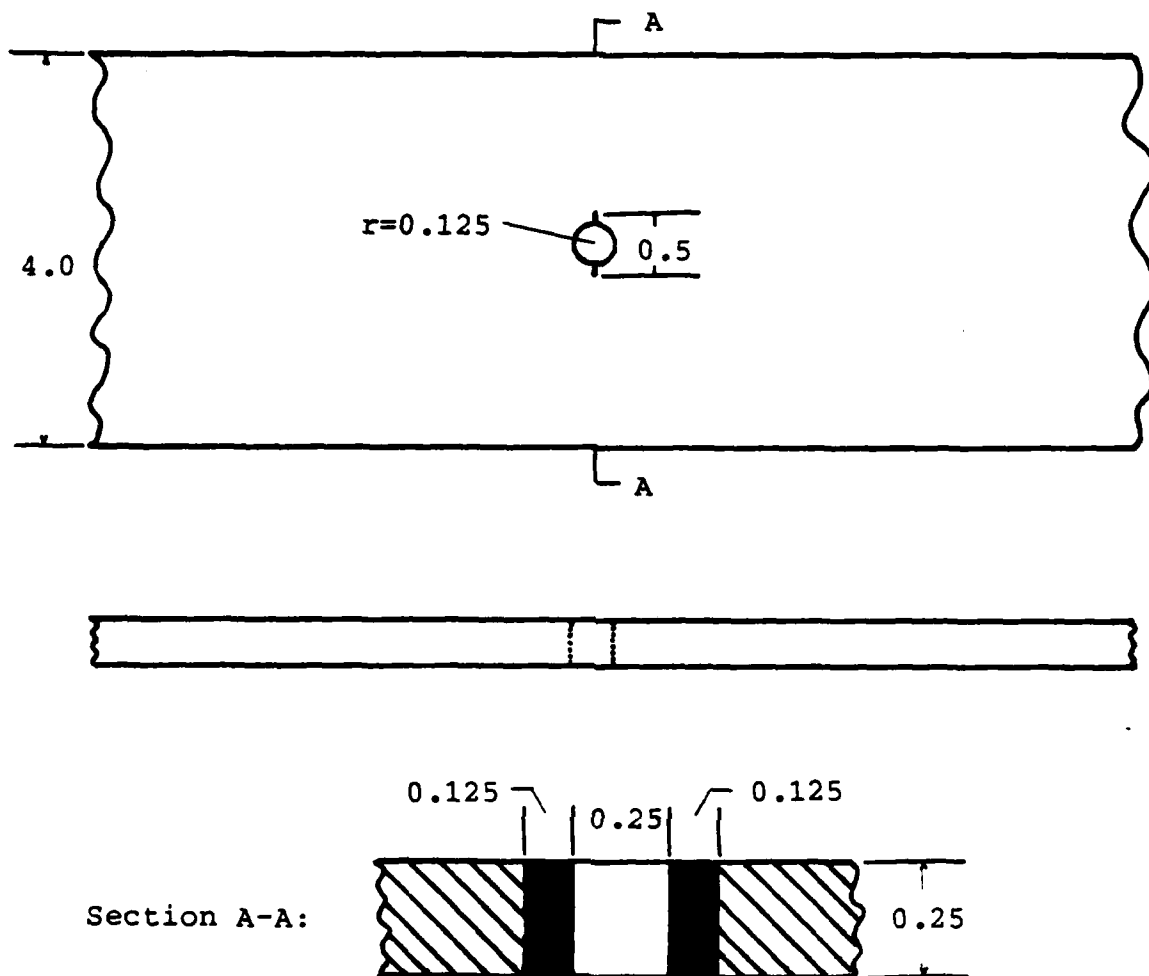
In order to simulate the output of an IAT system, reasonable values for input parameters had to be defined. This was done by creating a scenario based on realistic aircraft flight conditions.

#### Scenario

The Aircraft. The aircraft selected for study was a generic front-line NATO fighter with a design limit stress of 40 ksi. The structural location analyzed by the IAT program was a four inch wide, one-quarter inch thick panel of 2024-T3 aluminum alloy, with a one-quarter inch diameter fastener hole in the center of the plate (see Figure 1). The structure had incurred fatigue damage at the hole represented by a pair of radial through-the-thickness cracks, each one-eighth inch long.

Although a lower stress level and smaller flaw size would have probably been more applicable to future aircraft, the major reasons for selecting the above values were: (1) resource costs that limited simulated aircraft lives to an average less than 5000 flight hours, (2) the availability of data for older aircraft, and (3) compatability with an ongoing test program within the Flight Dynamics Laboratory.

The Load History. The loading environment for the aircraft under study was represented by actual flight loads data recorded from approximately 150 consecutive flights of



Note: All dimensions are in inches.

Figure 1. Structural Geometry

a high performance NATO aircraft (28). Actual mission profiles are sensitive and cannot be described here. The flight history included air-to-ground, air-to-air, photo-reconnaissance, and non-tactical maneuvers. In all cases except air-to-ground weapons delivery, gross weight was assumed to decrease linearly from take-off until landing (28). In the air-to-ground mode, store weights were subtracted immediately when dropped.

The original load history described above was assumed to completely represent 150 flight hours of the "actual" loading environment. In that way, a convenient baseline was available with which to compare analytical results.

The IAT Device. Instead of selecting a specific IAT device, an exceedance curve was generated from the original load history. Such a curve, shown in Figure 2, is a common output of several IAT hardware devices. An exceedance curve represents the cumulative number of peak loads that exceed predetermined levels of load or stress. Since data are collected only a finite number of levels, the curve will generally appear as a step function.

Exceedance curve generation involves two major simplifications of the original load history -- the truncation of intermediate loads based on preset measurement levels, and the loss of information concerning the sequence in which the flight loads occurred (1). The effects of these two simplifications depend on the load history itself.

Since the actual load history is never known, there is no knowledge of just how much error is introduced by the simplifications.

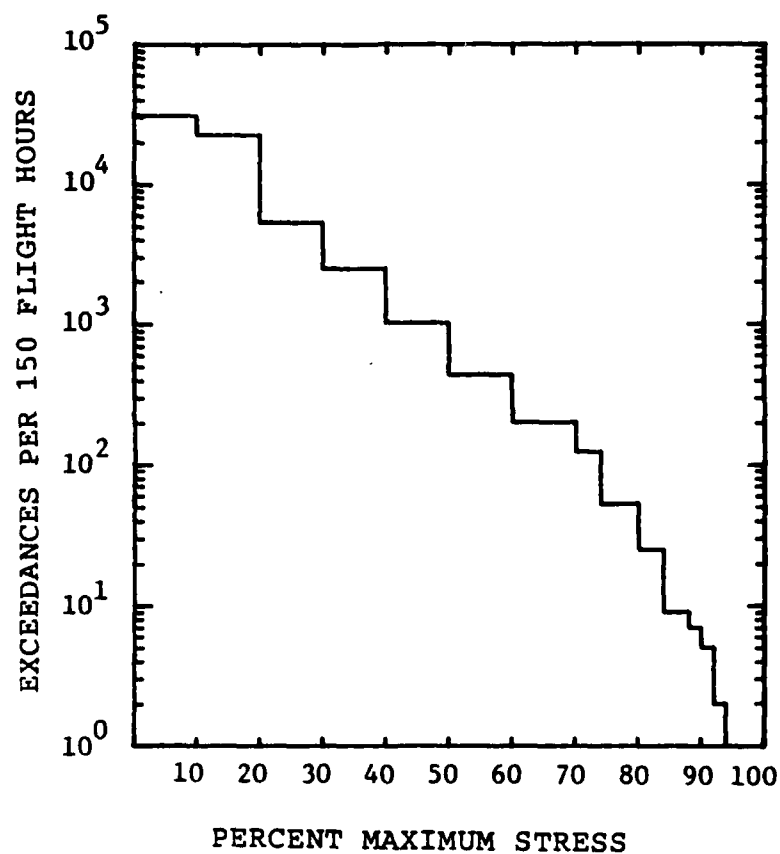


Figure 2. Exceedance Curve for Baseline Load History

The Figure 2 exceedance curve was selected to be compatible with a current AFWAL (Air Force Wright Aeronautical Laboratories) study on the reconstitution of an original load history based on IAT data (12). The curve represents the original load history discussed above. Four additional load histories were generated from the same exceedance curve using current Air Force cycle counting techniques.

Since the exceedance curve does not provide information concerning the sequence of recorded flight loads, the load cycles must be defined using a reconstitution algorithm. Two popular types of cycle definition schemes are rainflow counting and range-mean-pair counting (11). Table 1 shows the techniques used to develop the various load histories.

Table 1: Selected Load Histories

Variation	Generation Technique
Baseline	Actual cycle-by-cycle recorded data
RF2	Reconstituted by 0.2g rainflow count
RMP1	Reconstituted by 0.1g range-mean-pair count
RMP1F	Reconstituted by 0.1g range-mean-pair count into flight-by-flight load sequence
RMP2	Reconstituted by 0.2g range-mean-pair count

Theoretically, the exceedances for each load history should be identical. Due to the complexity of reconstitution techniques, there are subtle differences between the variations. Table 2 shows the resulting exceedance curve in tabular form for each of the load history variations.

Table 2: Exceedances for Each Load History Variation

Percent Design Limit Stress	Number of Exceedances (Peaks Only) Per 150 Flight Hours				
	Baseline	RF2	RMP1	RMP1F	RMP2
0	30795	31015	31015	30915	31015
10	30792	30997	31011	30911	30931
20	22473	22605	22604	22530	21115
30	5335	7139	5363	5343	4029
40	2465	2028	2478	2469	1885
50	1017	1023	1023	1017	943
60	438	523	440	438	336
70	201	165	201	201	137
74	122	90	122	122	82
80	52	52	52	52	42
84	25	25	25	25	19
88	9	9	9	9	8
90	7	9	7	7	3
92	5	5	5	5	3
94	2	5	2	2	1
96	1	1	1	1	1

Life Prediction Model. Life predictions were generated using the Air Force's CRACKS4 computer code, written by Engle (11). Inputs to the program are material properties, structural geometry, stress levels, and flight loads. Based on these values, the program models the growth of a structural crack using a cycle-by-cycle analysis. In the case of this simulation, each analysis incorporated between 500 thousand and two million load cycles before the structure failed. The CRACKS4 program and its capabilities are extensive. Please refer to Appendix B and to Reference 14 if additional information is required.

#### Simulation Procedure

Aircraft inspection intervals are based on the time required for an assumed structural flaw to grow to failure under specified loading conditions. Currently, the analysis is deterministic. If a parameter is unknown, an average or "conservative" value is used. Since the arbitrary selection of parameter values introduces uncertainty, safety factors ensure that inspections are conducted often enough to prevent major structural failures. Figure 3 illustrates the current deterministic IAT and Force Structural Maintenance philosophy (4: Sec 4,4-9).

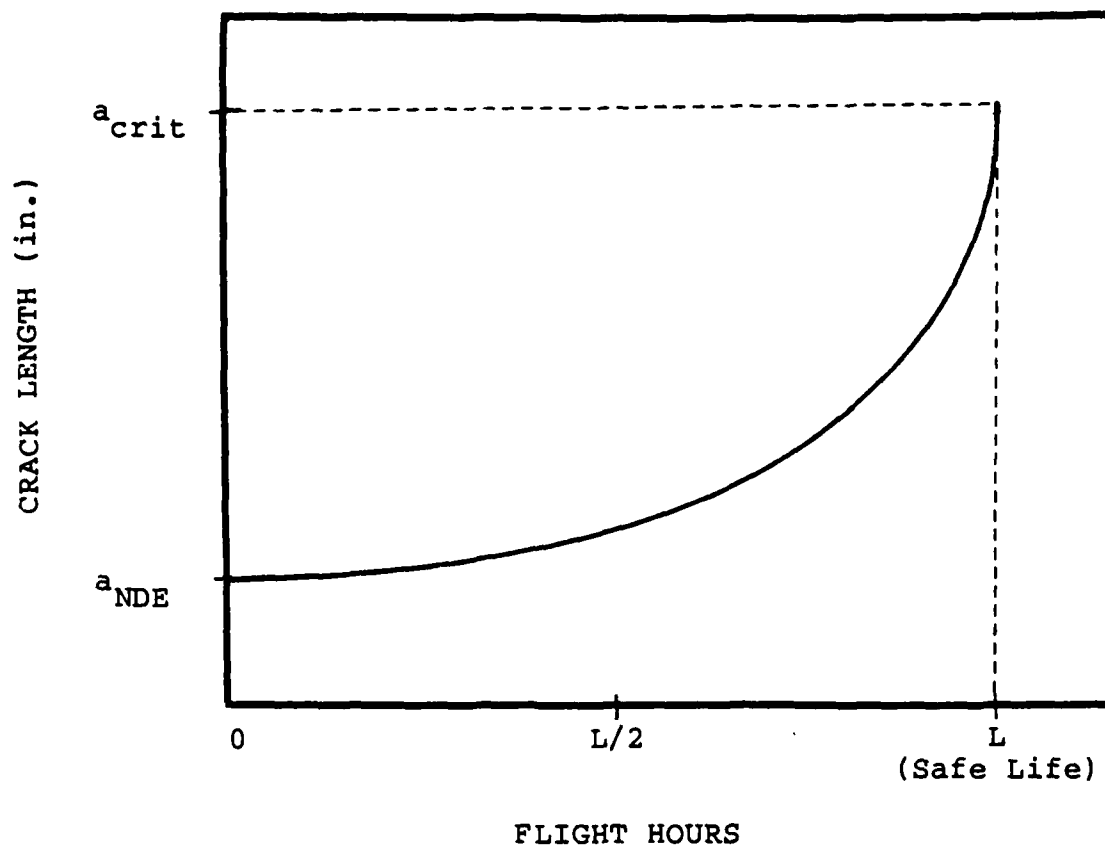


Figure 3. Determination of an Inspection Interval

The smallest crack size which should have been reliably found during the last non-destructive inspection becomes the assumed flaw size ( $a_{NDE}$ ). The flaw then "grows" analytically according to the average rate expected for the appropriate structural material under the anticipated loading conditions. The time for the flaw to grow to failure under those conditions is called the "safe life". The prescribed depot-level inspection time is one half of the time required for the flaw to grow from the initial

assumed size to the critical size associated with safe life. After each inspection, the assumed initial flaw size is reset to reflect inspection results and repairs. Based on IAT data from the field, the recorded flight loads are compared to the anticipated loads, and the safe life is adjusted using the new values.

**Assumptions.** For a completely stochastic approach, each of the variables just discussed would be represented by a probability distribution and varied independently to produce a realistic distribution of safe lives (Figure 4).

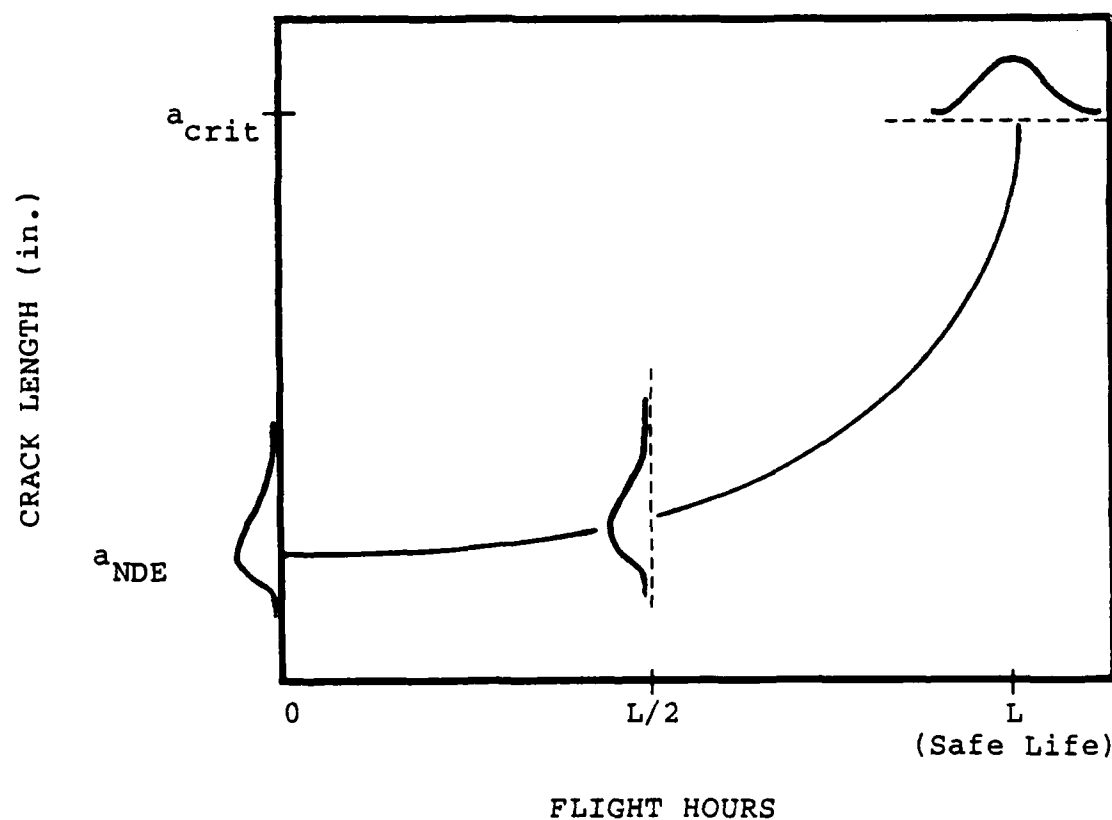


Figure 4. Stochastic Approach to Inspection Intervals

Due to the limited time and resources available for thesis work, the model was simplified to include twelve aircraft, represented by different values of material properties constants. Each aircraft was evaluated based on five different load history variations, represented by the baseline and reconstituted spectra. Finally, each aircraft was assigned three different gross weights, represented by stress levels of 38, 40, and 42 ksi. Consequently, there were 180 data points comprising the distribution of possible lives.

The following factors were held constant because of resource constraints. These factors are considered very important and should definitely be considered in future simulations. They were deleted only to achieve a reasonable scope for the thesis.

Data Capture Rate. IAT system limitations and malfunctions cause some of the data for aircraft flight loads to be lost. A broken wire, lightening strike, or mechanical failure could cause the IAT device to stop gathering data. Since data are only collected from the device periodically, problems can go undiscovered for days or weeks. In addition, data can be lost during shipment of cassettes and tapes from the flight line to the processing center. IAT programs vary greatly in scope and complexity (17:29) and therefore, the amount of meaningful data provided by the system varies as well. The typical data capture rate

for an IAT hardware device is currently in the range of 70 to 95 percent (1; 4: Sec 5,72).

Initial Flaw Size. As was already discussed, the assumed initial flaw size ( $a_{NDE}$ ) is arbitrarily set to the length of the smallest detectable crack for the previous inspection. The probability that a structural crack is just under the detectable size is not high, but that assumption is made to ensure that all aircraft have a reasonable chance of reaching the next inspection. There is also a chance that a flaw larger than the inspection size exists and was overlooked during the inspection. That probability is also low, and it is accounted for by the IAT safety factor.

The eventual transition of IAT from a deterministic process to the proposed stochastic approach cannot occur without a reasonable understanding of the initial flaw distribution. However, since all current IAT systems use the  $a_{NDE}$  initial flaw assumption, a comparison of various IAT systems is possible based on a single initial flaw size.

Variables. Three major variables were selected to provide a realistic simulation of the aircraft environment within thesis resource constraints. These variables were (1) material properties, (2) the load history, and (3) stress level.

Material Properties. To determine the appropriate crack growth characteristics for the structural material, data were obtained from a 1978 study of fatigue crack

propagation done at Purdue University (29). These data represent a single production batch of 2024-T3 aluminum tested under highly controlled conditions, and provide an excellent database for determining the underlying distributions which govern fatigue crack propagation. The data do not necessarily represent the variety expected of a fleet-wide cross section of material properties.

The Purdue data resulted from 68 replicate constant amplitude crack growth rate tests. All test specimens had identical starting geometries, and each received the same carefully controlled loading. For each test, 164 crack length measurements were recorded. The composite plot of these test results is shown in Figure 5.

The scatter among the 68 replicate curves is noteworthy because a single value is currently used to represent the "typical" curve. Even though the average of all of the curves can be calculated, and a typical curve can be identified, a single value can never represent all of the possible outcomes. Unless the variation shown in Figure 5 is accounted for, material properties data will only provide a rough estimate of what can be expected to happen.

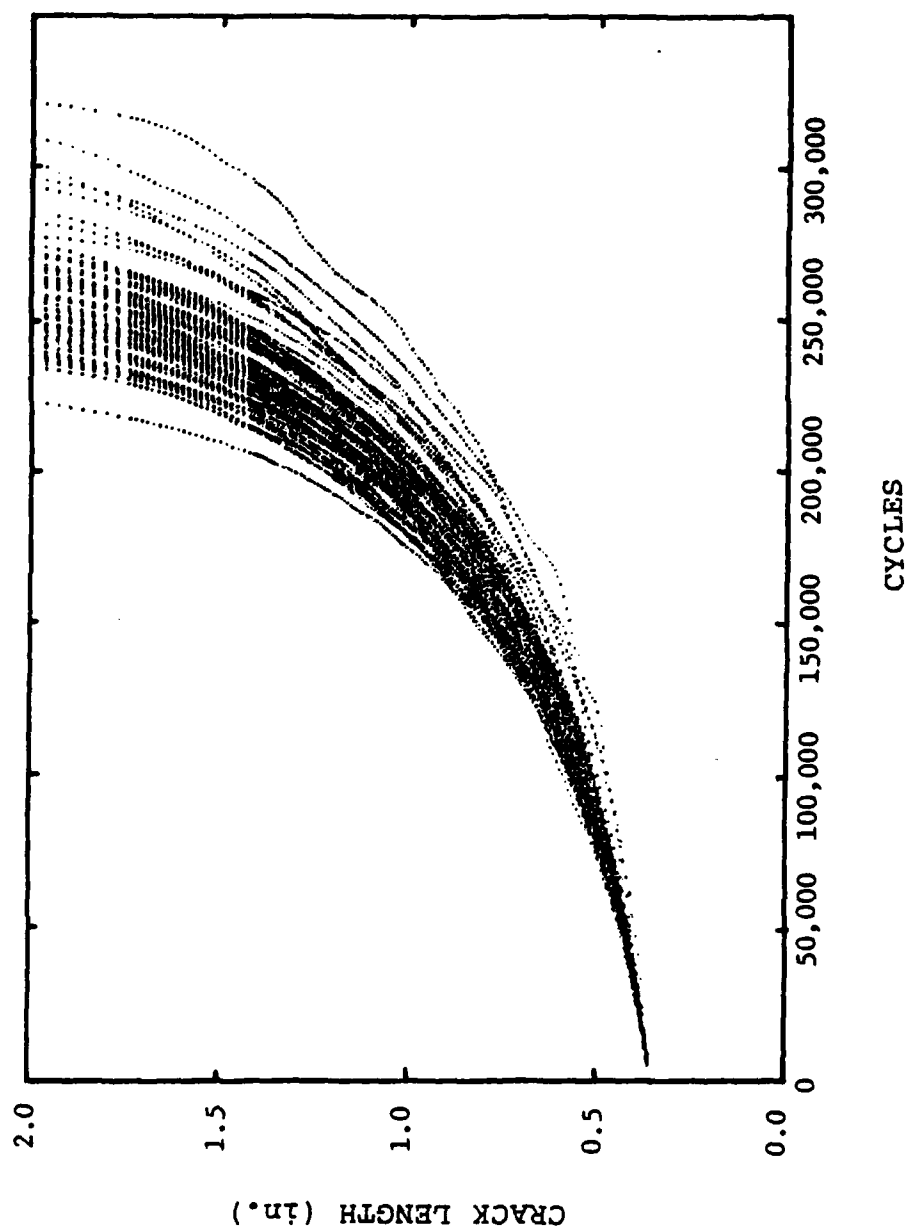


Figure 5. Crack Growth Curves (68 Curves, 11,152 Points)

The following paragraphs summarize the procedure used to convert the raw crack length vs cycles data into the format appropriate for simulation. The process was actually a simulation in itself. For a complete description of the material properties simulation, please refer to Appendix A.

To transform the crack growth data into a form useful for analysis, the derivative of each curve was calculated. Crack growth rates (known as  $da/dn$ ) for each specimen were approximated by the modified secant method. Growth rates were then plotted against the stress intensity factor,  $\Delta K$ , as shown in Figure 6.

Only the linear portion of the  $da/dn$  curves, between  $\Delta K$  values of 9 and 18, were of interest. Values outside of this range were deleted. The slope and intercept of every curve was determined by a least squares linear regression, as well as the overall slope and intercept of the composite curve (8228 data points). The linear regression of  $da/dn$  data is often called a "Paris" fit (24).

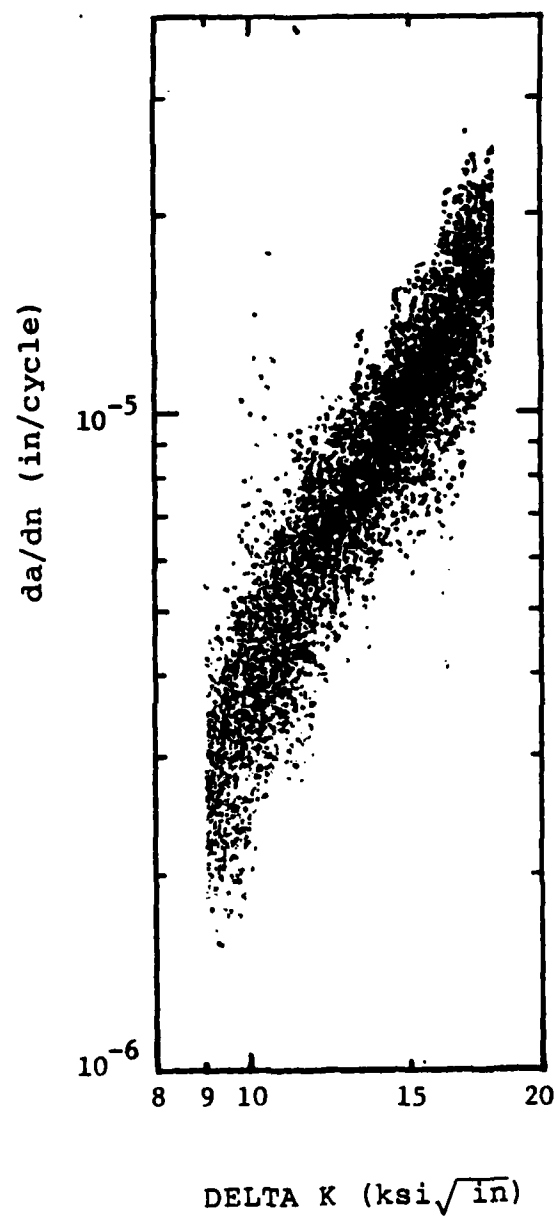


Figure 6. Crack Growth Rate Curves (Linear Range Only)

A CRACKS4 analysis requires more information than is provided by simply knowing the slope and intercept of the crack growth rate curve. Therefore, the Walker crack growth rate equation (30) was selected for use and derived from the least squares equation by fixing the "collapsing factor", m.

$$\frac{da}{dn} = C \left[ \Delta K \left( (1-R)^{m-1} \right) \right]^N \quad (1)$$

where

C, N, m = Empirically derived material constants  
 $\Delta K$  = Stress intensity factor  
R = Stress ratio

$\frac{da}{dn}$  = Crack growth rate

Once the Walker slope and intercept values were determined, their underlying probability distributions had to be found. The slope, N, was evaluated first and passed goodness of fit testing for a normal distribution. Next, values for the intercept, C, were evaluated and determined to be lognormally distributed. Based on the probability density functions, values for both C and N were randomly generated and entered into a simulation to see if the lives of the original specimens could be reasonably predicted. Results indicated that values for the slope and intercept of a particular line were highly correlated, and that a random pairing of C and N values consistently lead to huge errors.

The new approach was to calculate C based on a particular value of the slope, N, and the covariance between N and C. A third distribution was generated with the assumption that error terms about a regression line are normally distributed with a mean of zero. Once values for the slope and error term were generated, the appropriate value for C was completely and accurately specified.

Specimen lives predicted by the material simulation were about five percent conservative (too short) when compared to data from the Purdue study. Subsequent analysis showed that over four and one-half percent of the error was due to the regression, and only about one-half percent was due to the simulation process. Since crack growth rate curves are seldom perfectly linear, the regression error was considered quite good. A five percent error is very small compared to normal fatigue variability, and a slightly conservative error is often desired. Thus, the material properties simulation was considered valid.

Load Histories. Figure 2 showed the exceedance curve generated by the IAT device under study. The curve is reproduced here as Figure 7 and indicates the number of flight loads which exceeded specified levels of normal acceleration. After data collection, normal accelerations were converted to stresses and expressed as a percent of design limit stress. The exceedance curve can be thought of as a cumulative probability distribution function.

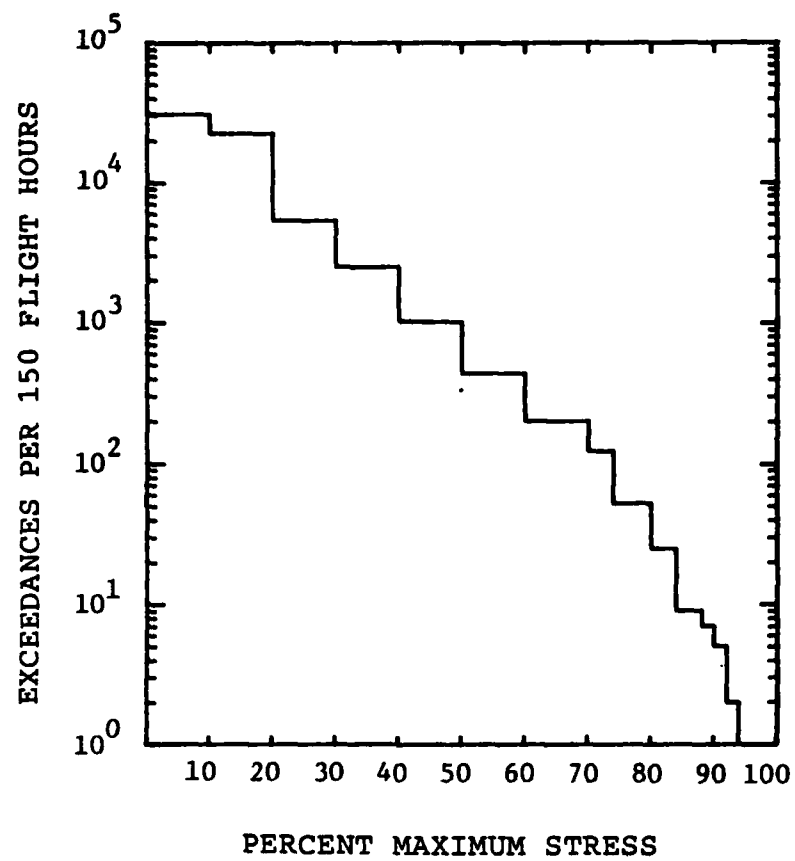


Figure 7. Exceedance Curve for Baseline Load History

Figure 7 was used to generate all load history variations used in this study. Ideally, each of the variations should have produced the same predictions of structural lives. However, the sources of error discussed earlier (truncation and sequence) influence the validity of reconstituted spectra. The baseline load history and four reconstituted variations were used to represent the variability introduced by the IAT measurement techniques.

Stress Levels. Variations in design limit stress were included to represent the effects of different aircraft gross weights. Gross weight is difficult to measure on a real time basis. Most values for weight are estimated based on pilot log reports and stores information. Since weight is extremely important for converting normal accelerations (g's) to structural stress levels, three values for limit stress were used to represent inaccuracies in weight estimates. These values also help incorporate differences in stress levels due to variations in the mach number and altitude of the aircraft during maneuvers (20). A stress of 40 ksi represented the expected aircraft gross weight. Deviations of plus and minus five percent were used to represent the effects of typical gross weight variations on the life prediction process (6).

The Simulation. The simulation was conducted using AFIT's Harris 800 mini-computer. A CRACKS4 analysis was run using the baseline load history with the following inputs:

Analysis Equation:	Walker
Retardation Model:	Willenborg
Yield Strength:	50 ksi
Fracture Toughness:	65 ksi $\sqrt{\text{in}}$
Yield Zone:	Plane Stress
Plate Width:	4.0 inches
Hole Radius:	0.125 inches
Initial Flaw Size:	0.125 inches (Each Side of Hole)
Geometric Factors:	Beta (Finite Width Correction)
	Bowie (2 Cracks From Circular Hole)

For the baseline aircraft life, the above information was input into the CRACKS4 program along with a stress level of 40 ksi. Average material crack growth properties obtained from the Purdue study ( $C=7.403 \times 10^{-9}$ ,  $N=2.631$ ) were used in the Walker equation along with the fixed value of 0.682 for  $m$ . These data yielded a baseline life of approximately 4700 flight hours. The baseline life represented the best deterministic estimate of the aircraft safe life when the loading history and stress levels were completely known. Dividing by the safety factor of 2.0 produced required depot-level inspection interval of 2350 flight hours. The anticipated crack length at that inspection was 0.282 inches on each side of the hole.

After the baseline values were determined, values for each variable of interest were introduced and aircraft lives were simulated. Table 3 lists values generated for each variable, and used as inputs for the simulation.

Table 3: Random Variable Inputs to the Simulation

Maximum Applied Stress	Load History Variation	Material Properties	
		C	N
38 ksi	Baseline	3.727E-9	2.891
40 ksi	RF2	8.204E-9	2.594
42 ksi	RMP1F	7.991E-9	2.627
	RMP1	1.136E-8	2.448
	RMP2	5.597E-9	2.784
		1.984E-8	2.234
		3.607E-9	2.961
		1.105E-8	2.446
		2.653E-9	3.053
		7.462E-9	2.608
		1.545E-9	3.275
		6.462E-9	2.705

All combinations of the above variables were analyzed, yielding 180 values for aircraft life, and 180 values for the crack length present at the 2350 flight hour inspection. These values were then evaluated to determine the resulting fleet-wide distribution.

### Summary

In order to conduct a valid simulation, reasonable values for input parameters had to be selected. Material crack growth constants were determined from 68 replicate constant amplitude fatigue tests conducted by Reference 29. Five load history variations were developed from a common exceedance curve using current USAF cycle counting techniques. Finally, aircraft gross weight variations were represented by the expected value for design limit stress, along with deviations of plus and minus five percent.

#### IV. Results

The simulation produced a mean aircraft residual life of 4764 flight hours, based on the initial flaw assumptions discussed in Chapter III. Of the 180 combinations of structural material properties, stress histories, and stress levels evaluated, only five led to the failure of an aircraft before the 2350 hour depot-level inspection. Although that number may appear high, it is important to remember that (1) The structures under study do not represent new aircraft. The one-eighth inch cracks assumed to be present at critical fastener holes represent the post-inspection reset size ( $a_{NDE}$ ) based on inspection capabilities. (2) The initial flaw assumption is very severe. The probability of such a flaw existing in a single aircraft is quite low, and the chances that the flaw is present in every aircraft in the fleet are definitely negligible. (3) The intent of the simulation presented in this thesis was to provide a means by which various IAT systems can be directly compared with one another. The focus was on relative failure rates before inspection, not the absolute number given above.

Based on expected aircraft gross weight, the maximum stress was calculated to be 40 ksi at the structural location of interest. Using this value for stress, along with the average material properties expected for 2024-T3

aluminum and the actual recorded flight load history, a baseline curve for residual aircraft life was determined.

The baseline curve was generated by CRACKS4 analysis as were all other curves in the simulation. The Walker constants used to specify crack growth rates were obtained by a single least squares regression for all data discussed in Appendix A. These data are shown in Figures 6 and A1. The resulting values were:  $C = 7.403 \times 10^{-9}$ ,  $N = 2.631$ . The baseline curve is shown in Figure 8.

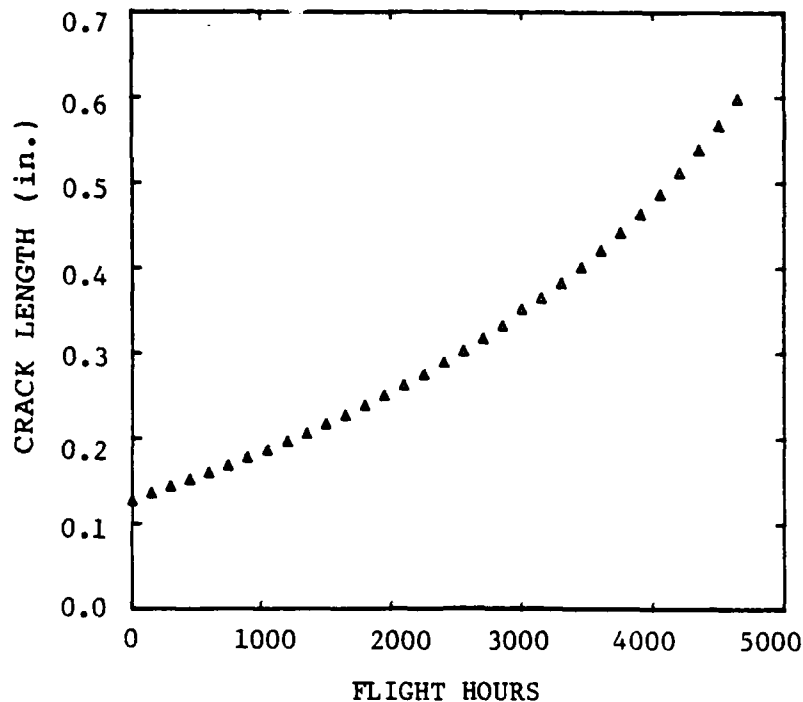


Figure 8. Baseline Curve Representing Expected Crack Growth Behavior

Once the baseline curve was generated, the expected aircraft residual life was defined to be the time required for failure, or 4696.82 flight hours. For convenience, the life was rounded to 4700 hours. The depot-level inspection time then became 2350 hours, or one-half lifetime. Data for structural crack lengths were only available in increments of 150 flight hours, so the crack size at inspection was interpolated between values obtained at 2250 and 2400 hours. Using this procedure, the expected crack length at inspection was determined to be 0.282 inches.

The baseline curve represents the best deterministic estimate available for aircraft residual life. Since the load history and structural geometry were completely known, only material constants were approximated. Therefore, the baseline curve was used to represent the true behavior of the average aircraft in order to assess the validity of simulation results.

#### Simulation Output Data

Simulation results are listed in Tables 4 through 10 on the next 7 pages. Table 4 provides a summary of all results, while Tables 5 through 10 list individual test results by stress level.

Table 4: Summary of Simulation Results by Stress Level

MAXIMUM STRESS	LIFE			INSPECTION CRACK LENGTH		
	Mean (Flt Hrs)	Standard Deviation	No. of Points	Mean (Inches)	Standard Deviation	No. of Points
38 ksi	5703.69	1413.64	60	0.271	0.050	60
40 ksi	4703.78	1210.90	60	0.302	0.061	59
42 ksi	3883.99	1033.70	60	0.333	0.071	56
All Tests	4763.82	1432.12	180	0.301	0.066	175
Expected	4696.82	-----	1	0.282	-----	1

Notes:

Five structures failed before the scheduled inspection.

Table 5: Aircraft Lives in Flight Hours, Based on a Maximum Stress of 38 ksi

Material Constants		Load History							
C	N	BASELINE	RF2	RMPLF	RMP1	RMP2	Mean	Std Dev	
3.727E-9	2.891	5146.75	4276.38	5297.21	5620.27	6678.09	5403.74	868.79	
8.204E-9	2.594	5896.62	5026.26	6047.09	6220.18	7427.97	6123.62	862.01	
7.991E-9	2.627	5446.70	4576.33	5447.19	5770.25	6978.04	5643.70	867.93	
1.136E-8	2.448	6646.50	5776.14	6796.97	7120.03	8477.80	6963.49	981.79	
5.597E-9	2.784	4696.82	3976.43	4847.29	5020.37	6078.18	4923.82	757.76	
1.984E-8	2.234	7396.38	6526.02	7396.88	7719.93	9077.70	7623.38	926.20	
3.607E-9	2.961	4096.92	3376.53	4247.38	4570.44	5478.28	4353.91	765.47	
1.105E-8	2.446	6946.45	6076.09	7096.92	7419.98	8777.75	7263.44	981.79	
2.653E-9	3.053	4246.89	3376.53	4397.36	4720.42	5628.26	4473.89	814.70	
7.462E-9	2.608	6196.58	5326.21	6347.05	6670.10	7877.89	6483.57	924.58	
1.545E-9	3.275	3497.01	2776.62	3647.48	3970.54	4878.38	3754.01	765.47	
6.462E-9	2.705	5146.75	4426.36	5297.21	5620.27	6678.09	5433.74	821.44	
Mean:		5446.70	4626.32	5572.17	5870.23	7003.04			
Std Dev:		1208.30	1160.53	1187.53	1191.83	1360.85			

Notes:

Max: 9077.70      Average: 5703.69  
 Min: 2776.62      Std Dev: 1413.64

Table 6: Aircraft Lives in Flight Hours, Based on a Maximum Stress of 40 ksi

Material Constants		Load History								
C	N	BASELINE	PF2	RMPLF	RMPL	RMP2	Mean	Std Dev		
3.727E-9	2.891	4096.92	3376.53	4247.38	4570.44	5478.28	4353.91	765.47		
8.204E-9	2.594	4846.79	4126.40	4997.26	5170.34	6228.16	5073.79	757.76		
7.991E-9	2.627	4396.87	3826.45	4547.34	4720.42	5778.23	4653.86	712.50		
1.136E-8	2.448	5596.67	4876.28	5597.17	5920.22	6978.04	5793.68	764.49		
5.597E-9	2.784	3796.97	3226.55	3947.43	4120.51	5028.35	4023.96	654.10		
1.984E-8	2.234	6196.58	5476.19	6197.07	6520.13	7727.92	6423.58	823.26		
3.607E-9	2.961	3347.04	2776.62	3497.51	3670.59	4428.45	3544.04	597.52		
1.105E-8	2.446	5746.65	5026.26	5897.12	6070.20	7277.99	6003.64	815.64		
2.653E-9	3.053	3347.04	2776.62	3497.51	3820.56	4578.43	3604.03	663.01		
7.462E-9	2.608	5146.75	4426.36	5297.21	5470.30	6528.11	5373.75	757.76		
1.545E-9	3.275	2897.11	2326.70	2897.60	3220.66	3973.84	3063.18	602.39		
6.462E-9	2.705	4246.89	3676.48	4397.36	4720.42	5628.26	4533.88	719.13		
Mean:		4471.86	3826.45	4584.83	4832.90	5802.84				
Std Dev:		1049.83	988.64	1035.37	1029.42	1184.74				

Notes:

Max: 7727.92  
Min: 2326.70  
Average: 4703.78  
Std Dev: 1210.90

Table 7: Aircraft Lives in Flight Hours, Based on a Maximum Stress of 42 ksi

Material Constants		Load History						Mean	Std Dev
C	N	BASELINE	RF2	RMPLF	RMP1	RMP2			
3.727E-9	2.891	3347.04	2776.62	3497.51	3670.59	4428.45	3544.04	597.52	
8.204E-9	2.594	3946.94	3376.53	4097.41	4270.49	5178.33	4173.94	654.10	
7.991E-9	2.627	3646.99	3076.57	3797.46	3970.54	4728.40	3843.99	597.52	
1.136E-8	2.448	4546.84	3976.43	4697.31	4870.39	5928.21	4803.84	712.50	
5.597E-9	2.784	3197.06	2626.65	3197.55	3370.64	4128.50	3304.08	539.86	
1.984E-8	2.234	5146.75	4576.33	5297.21	5470.30	6528.11	5403.74	712.50	
3.607E-9	2.961	2747.14	2326.70	2747.63	3070.68	3678.57	2914.14	502.39	
1.105E-8	2.446	4846.79	4126.40	4847.29	5020.37	6078.18	4983.81	702.06	
2.653E-9	3.053	2747.14	2326.70	2897.60	3070.68	3828.55	2974.13	551.34	
7.462E-9	2.608	4246.89	3676.48	4397.36	4570.44	5478.28	4473.89	654.10	
1.545E-9	3.275	2297.21	1876.77	2447.68	2620.76	3228.64	2494.21	494.37	
6.462E-9	2.705	3497.01	2926.60	3647.48	3820.56	4578.43	3694.02	597.52	
Mean:		3684.48	3139.06	3797.46	3983.04	4815.89			
Std Dev:		888.71	822.59	895.30	880.23	1036.02			

Notes:

Max: 6528.11      Average: 3883.99  
Min: 1876.77      Std Dev: 1033.70

Table 8: Crack Length (inches) at 2350 Hour Depot-Level Inspection,  
Based on a Maximum Stress of 38 ksi

Material Constants		Load History						
C	N	BASELINE	RF2	RMP1F	RMP1	RMP2	Mean	Std Dev
3.727E-9	2.891	0.270	0.314	0.264	0.254	0.229	0.266	0.031
8.204E-9	2.594	0.254	0.283	0.251	0.243	0.223	0.251	0.022
7.991E-9	2.627	0.268	0.302	0.264	0.255	0.232	0.264	0.025
1.136E-8	2.448	0.239	0.260	0.236	0.231	0.213	0.236	0.017
5.597E-9	2.784	0.293	0.342	0.286	0.274	0.245	0.288	0.035
1.984E-8	2.234	0.232	0.248	0.230	0.226	0.210	0.229	0.014
3.607E-9	2.961	0.319	0.390	0.309	0.292	0.258	0.314	0.049
1.105E-8	2.446	0.234	0.253	0.231	0.226	0.209	0.231	0.016
2.653E-9	3.053	0.309	0.380	0.299	0.283	0.250	0.304	0.048
7.462E-9	2.608	0.245	0.271	0.241	0.235	0.216	0.242	0.020
1.545E-9	3.275	0.360	0.485	0.344	0.316	0.272	0.355	0.080
6.462E-9	2.705	0.271	0.309	0.266	0.257	0.233	0.267	0.028
Mean:		0.275	0.320	0.268	0.258	0.233		
Std Dev:		0.039	0.070	0.035	0.029	0.020		

Notes:

Max: 0.485  
Min: 0.209  
Average: 0.271  
Std Dev: 0.050

Table 9: Crack Length (inches) at 2350 Hour Depot-Level Inspection,  
Based on Maximum Stress of 40 ksi

Material Constants		Load History						Mean	Std Dev
C	N	BASELINE	RF2	RMPLF	RMP1	RMP2			
3.727E-9	2.891	0.307	0.367	0.299	0.285	0.252	0.302	0.042	
8.204E-9	2.594	0.280	0.317	0.275	0.266	0.241	0.276	0.027	
7.991E-9	2.627	0.298	0.343	0.293	0.282	0.252	0.294	0.033	
1.136E-8	2.448	0.259	0.285	0.255	0.249	0.228	0.256	0.020	
5.597E-9	2.784	0.335	0.403	0.326	0.309	0.271	0.329	0.048	
1.984E-8	2.234	0.248	0.267	0.246	0.241	0.222	0.245	0.016	
3.607E-9	2.961	0.377	0.482	0.363	0.337	0.290	0.370	0.071	
1.105E-8	2.446	0.253	0.277	0.250	0.243	0.223	0.249	0.019	
2.653E-9	3.053	0.365	0.472	0.351	0.326	0.282	0.359	0.071	
7.462E-9	2.608	0.269	0.301	0.264	0.256	0.232	0.264	0.025	
1.545E-9	3.275	0.455	Failed	0.428	0.381	0.317	0.395	0.060	
6.462E-9	2.705	0.304	0.354	0.297	0.285	0.254	0.299	0.036	
Mean:		0.313	0.352	0.304	0.288	0.255			
Std Dev:		0.061	0.124	0.055	0.043	0.030			

Notes:

Max: 0.482  
Min: 0.222  
Average: 0.302  
Std Dev: 0.061

Table 10: Crack Length (inches) at 2350 Hour Depot-Level Inspection,  
Based on a Maximum Stress of 42 ksi

Material Constants		Load History						Mean	Std Dev
C	N	BASELINE	RF2	RMPLF	RMP1	RMP2			
3.727E-9	2.891	0.354	0.440	0.343	0.323	0.281	0.348	0.058	
8.204E-9	2.594	0.312	0.359	0.305	0.294	0.262	0.306	0.035	
7.991E-9	2.627	0.336	0.395	0.328	0.313	0.276	0.330	0.043	
1.136E-8	2.448	0.282	0.314	0.278	0.270	0.244	0.278	0.025	
5.597E-9	2.784	0.389	0.485	0.377	0.350	0.303	0.381	0.067	
1.984E-8	2.234	0.267	0.290	0.264	0.258	0.236	0.263	0.019	
3.607E-9	2.961	0.456	Failed	0.436	0.396	0.332	0.405	0.055	
1.105E-8	2.446	0.275	0.305	0.271	0.263	0.239	0.271	0.024	
2.653E-9	3.053	0.445	Failed	0.424	0.384	0.322	0.394	0.054	
7.462E-9	2.608	0.297	0.339	0.291	0.281	0.252	0.292	0.031	
1.545E-9	3.275	Failed	Failed	0.568	0.480	0.378	0.475	0.095	
6.462E-9	2.705	0.345	0.413	0.336	0.319	0.280	0.339	0.048	
Mean:		0.342	0.371	0.352	0.328	0.284			
Std Dev:		0.117	0.177	0.088	0.066	0.043			

Notes:

Max: 0.568  
Min: 0.236

Average: 0.333  
Std Dev: 0.071

All values for standard deviation were calculated using the unbiased estimator, which was determined from the following equation for variance (9:88):

$$s^2 = \{E(X^2) - [E(X)]^2\} [n/(n-1)] \quad (2)$$

where

$E(X)$  = Expected value (mean) of  $X$   
 $n$  = Sample size

which is equivalent to

$$s^2 = \frac{(X_i - \bar{X})^2}{n-1} \quad (3)$$

Calculations based on inspection crack lengths ignored structures which failed before reaching the 2350 hour inspection point. Deletion of the missing values from computations was appropriate for several reasons. (1) No reasonable values were available to substitute for the missing data. (2) Failure rates are accounted for by the distribution of lives, not crack lengths. (3) The failed structures will never reach the depot for inspection, so including them would bias the analytical results as compared to real world data.

## Analysis of Output Data

Determining Distributions. The first step in analyzing simulation output data was to plot histograms. The shape of a histogram can often indicate the type of underlying probability distribution which represents the behavior under study. Therefore, histograms were plotted at each stress level for both structural life and inspection crack length. These histograms are shown in Figures 9 through 14.

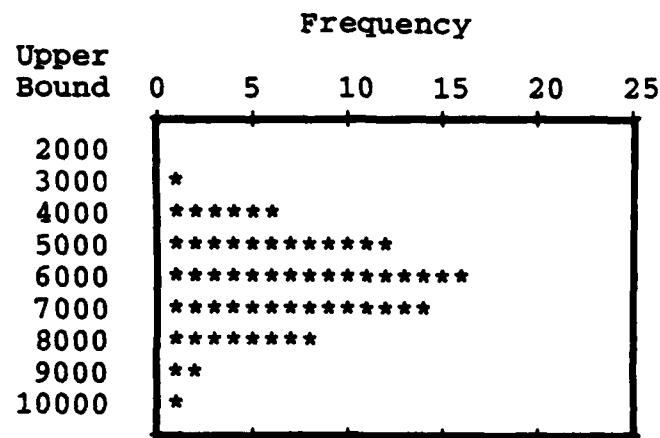


Figure 9. Histogram for Structural Lives at 38 ksi

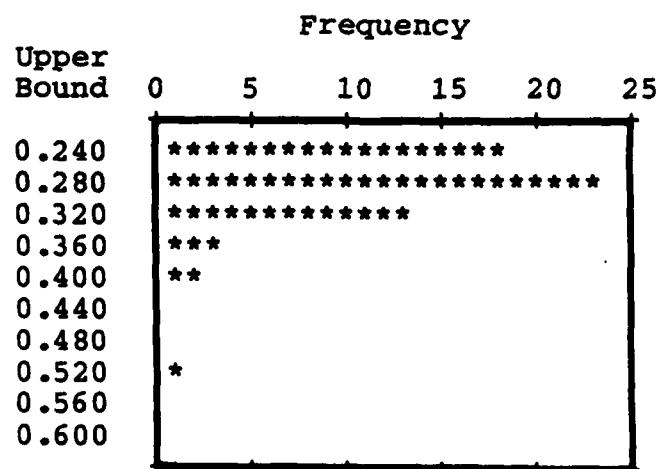


Figure 10. Histogram for Inspection Crack Lengths at 38 ksi

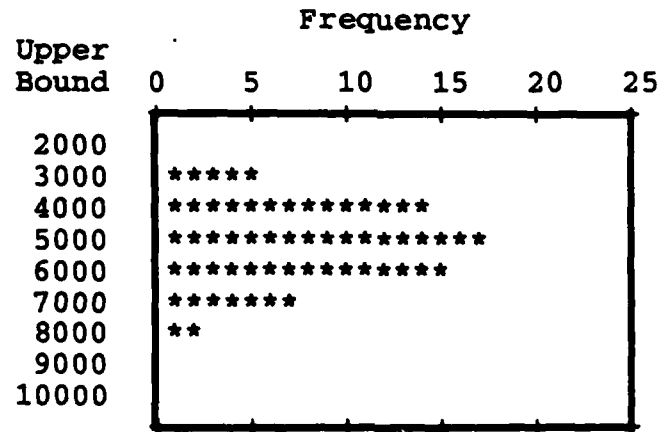


Figure 11. Histogram for Structural Lives at 40 ksi

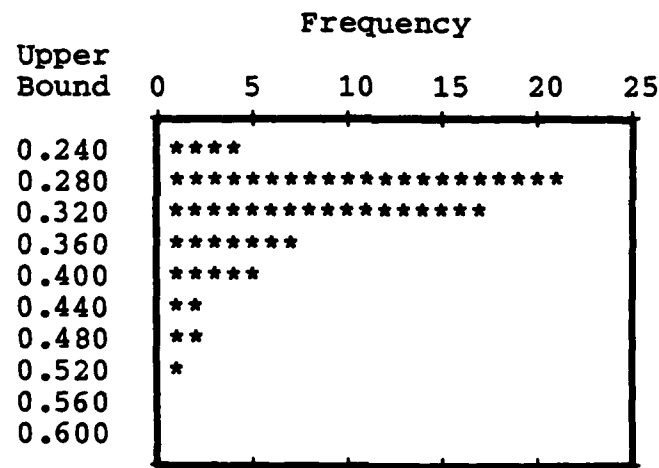


Figure 12. Histogram for Inspection Crack Lengths at 40 ksi

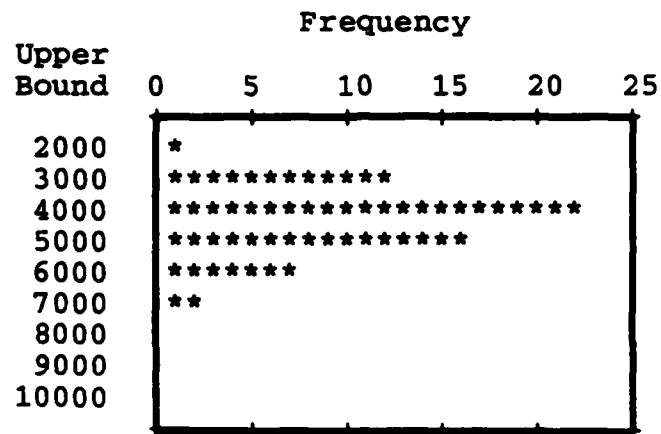


Figure 13. Histogram for Structural Lives at 42 ksi

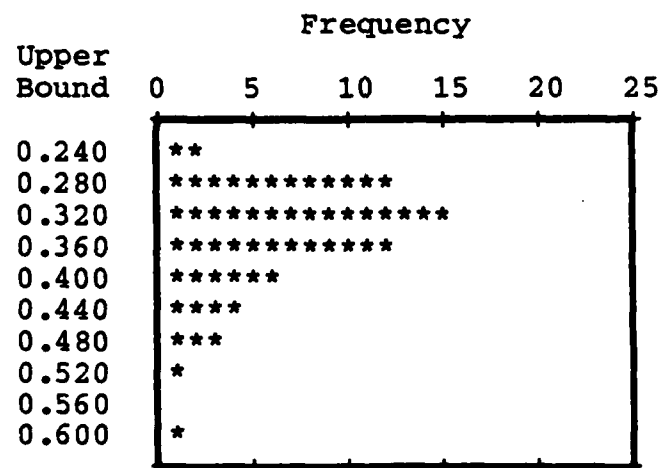


Figure 14. Histogram for Inspection Crack Lengths at 42 ksi

Based on the shape of the histograms, the distribution of lives appeared to be normal, while the distribution of crack lengths found during inspection appeared to be lognormal. Therefore, Chi-squared goodness of fit tests were accomplished. Instead of evaluating a lognormal distribution for crack length, a normal distribution was evaluated against the natural log of crack length. Results are the same, but the normal distribution was easier to work with. Tables 11 through 13 show the Chi-squared goodness of fit test results for structural lives. Tables 14 through 16 show similar test results for crack lengths.

The Chi-squared test statistic involves a comparison between the number of data points actually observed in a particular cell of the histogram (O), and the number of data points expected to be in that cell (E) for the distribution being evaluated. If the sum of Chi-squared statistics for all cells is less than the critical value associated with that number of cells, then the distribution provides an adequate fit of the data. The equation for Chi-squared is

$$\chi^2 = \frac{(O - E)^2}{E} \quad (4)$$

where

O = Number of observations in cell  
E = Number expected in cell

For all goodness of fit tests shown in this chapter, the level of significance was 0.05. The critical value for Chi-squared was 14.1 unless otherwise noted. The cell limits used for the Chi-squared tests do not correspond to the cell limits used to plot histograms. Cells used for goodness of fit testing were determined by using intervals of equal probability rather than equal width, as suggested by several sources (2:352). These intervals were calculated after the distribution shape was determined from the histograms. Note that the values for cell upper bounds in Tables 14 through 16 represent  $\ln(a)$ , and therefore have negative values.

Table 11: Chi-squared Fit for Normal Distribution of Lives at a Maximum Stress of 38 ksi

Cell	Upper Bound	Expected Number	Observed Number	Chi-squared Statistic
1	3891.40	6	5	0.167
2	4513.41	6	8	0.667
3	4962.94	6	6	0.000
4	5346.04	6	7	0.167
5	5703.69	6	6	0.000
6	6061.34	6	4	0.667
7	6444.44	6	5	0.167
8	6893.98	6	6	0.000
9	7515.98	6	8	0.667
10	Infinity	6	5	0.167
		60	60	2.667

Notes:

Mean = 5703.69

Std Dev = 1413.64

Table 12: Chi-squared Fit for Normal Distribution  
of Lives at a Maximum Stress of 40 ksi

Cell	Upper Bound	Expected Number	Observed Number	Chi-squared Statistic
1	3151.41	6	5	0.167
2	3684.20	6	9	1.500
3	4069.27	6	5	0.167
4	4397.42	6	7	0.167
5	4703.78	6	5	0.167
6	5010.14	6	5	0.167
7	5338.29	6	5	0.167
8	5723.36	6	6	0.000
9	6256.15	6	8	0.667
10	Infinity	6	5	0.167
		60	60	3.333

Notes:

Mean = 4703.78

Std Dev = 1210.90

Table 13: Chi-squared Fit for Normal Distribution  
of Lives at a Maximum Stress of 42 ksi

Cell	Upper Bound	Expected Number	Observed Number	Chi-squared Statistic
1	2558.79	6	5	0.167
2	3013.61	6	8	0.667
3	3342.33	6	6	0.000
4	3622.46	6	5	0.167
5	3883.99	6	8	0.667
6	4145.52	6	6	0.000
7	4425.65	6	3	1.500
8	4754.37	6	7	0.167
9	5209.19	6	6	0.000
10	Infinity	6	6	0.000
		60	60	3.333

Notes:

Mean = 3883.99

Std Dev = 1033.70

Table 14: Chi-squared Fit for Normal Distribution of  
Ln(Crack Length) at a Maximum Stress of 38 ksi

Cell	Upper Bound	Expected Number	Observed Number	Chi-squared Statistic
1	-1.535	6	3	1.500
2	-1.462	6	8	0.667
3	-1.409	6	9	1.500
4	-1.364	6	9	1.500
5	-1.322	6	6	0.000
6	-1.280	6	6	0.000
7	-1.235	6	3	1.500
8	-1.182	6	4	0.667
9	-1.109	6	6	0.000
10	Infinity	6	6	0.000
		60	60	7.333

Notes:

Mean = -1.322

Std Dev = 0.166

Table 15: Chi-squared Fit for Normal Distribution of  
Ln(Crack Length) at a Maximum Stress of 40 ksi

Cell	Upper Bound	Expected Number	Observed Number	Chi-squared Statistic
1	-1.458	5.9	4	0.612
2	-1.375	5.9	9	1.629
3	-1.316	5.9	8	0.747
4	-1.265	5.9	7	0.205
5	-1.217	5.9	5	0.137
6	-1.169	5.9	7	0.205
7	-1.118	5.9	4	0.612
8	-1.059	5.9	3	1.425
9	-0.976	5.9	5	0.137
10	Infinity	5.9	7	0.205
		59.0	59	5.915

Notes:

Mean = -1.217

Std Dev = 0.188

One structure failed before the scheduled inspection.

Table 16: Chi-squared Fit for Normal Distribution of  
Ln(Crack Length) at a Maximum Stress of 42 ksi

Cell	Upper Bound	Expected Number	Observed Number	Chi-squared Statistic
1	-1.378	5.6	4	0.457
2	-1.289	5.6	8	1.029
3	-1.225	5.6	8	1.029
4	-1.171	5.6	5	0.064
5	-1.120	5.6	6	0.029
6	-1.069	5.6	2	2.314
7	-1.015	5.6	8	1.029
8	-0.951	5.6	3	1.207
9	-0.862	5.6	4	0.457
10	Infinity	5.6	8	1.029
		56.0	56	8.643

Notes:

Mean = -1.120                      Std Dev = 0.201

Four structures failed before inspection.

All data for life and ln(crack length) from individual stress levels easily passed goodness of fit testing for normal distributions. However, the utility of conducting goodness of fit tests for the entire group of 180 tests was uncertain, since only three stress levels were evaluated.

It was not clear whether adding the three individual normal distributions should necessarily result in another normal distribution. All three distributions of structural lives were based on the same set of material constants, and were therefore not independent samples. Fortunately, the degree of dependence is also a factor. In fact, "... if all variables were perfectly linearly dependent on the

first,  $X_i = a_i + b_i X_1$ , then the distribution of the sum of any number of them would have the same shape as the distribution of the first . . ." (3:253). Just such a relationship is discussed in Chapter IV. For every load history, the average structural life was a perfectly linear function of stress level. Therefore, adding the distributions of lives from each of the three stress levels must result in another normal distribution. The same approach was used for inspection crack lengths. Histograms for the entire sample of lives and crack lengths are shown in Figures 9 and 10.

Goodness of fit tests were conducted for the entire sample of 180 aircraft, with the assumption that the distribution of resulting values reasonably approximated the distribution expected for a larger number of stress levels. Tables 17 and 18 show goodness of fit results for all simulated aircraft lives and inspection crack lengths.

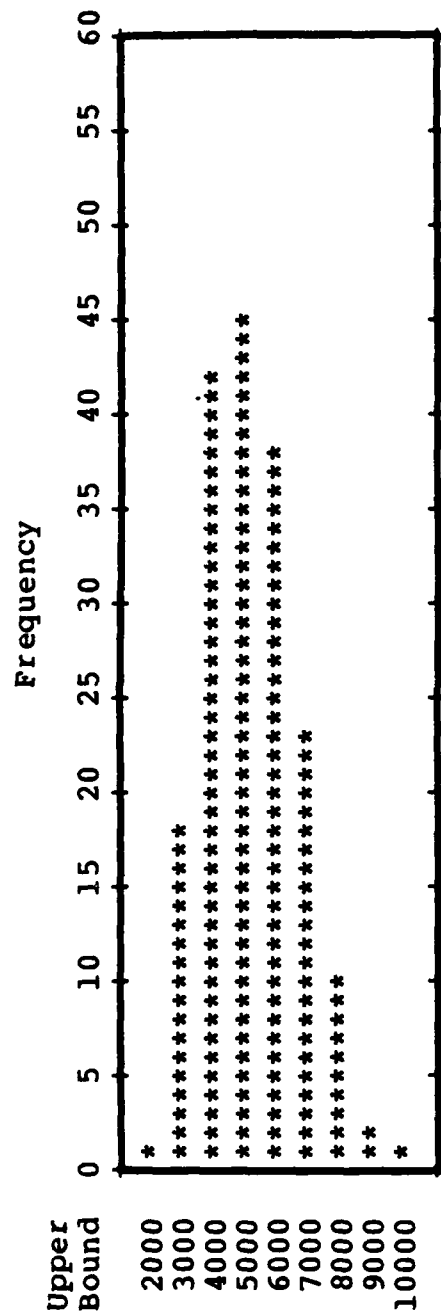


Figure 15. Histogram of Structural Lives (180 Points)

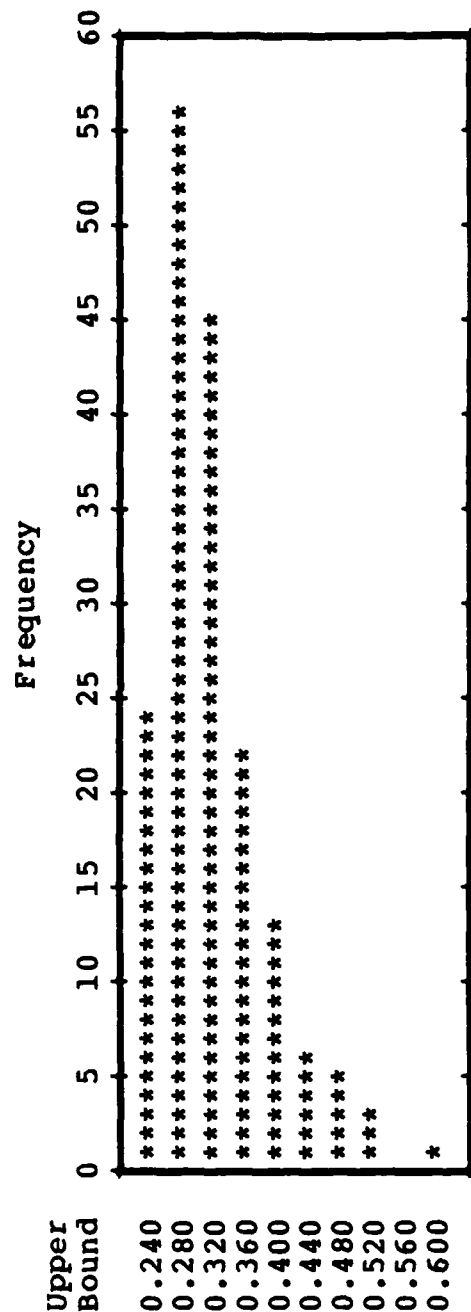


Figure 16. Histogram of Inspection Crack Lengths (175 Points)

Table 17: Chi-squared Fit for Normal Distribution  
of Lives -- All Tests

Cell	Upper Bound	Expected Number	Observed Number	Chi-squared Statistic
1	2927.84	18	19	0.056
2	3557.98	18	21	0.500
3	4013.39	18	21	0.500
4	4401.49	18	18	0.000
5	4763.82	18	19	0.056
6	5126.15	18	13	1.389
7	5514.25	18	19	0.056
8	5969.67	18	14	0.889
9	6599.80	18	15	0.500
10	Infinity	18	21	0.500
		180	180	4.444

Notes:

Mean = 4763.82

Std Dev = 1432.12

Table 18: Chi-squared Fit for Normal Distribution  
of Ln(Crack Length) -- All Tests

Cell	Upper Bound	Expected Number	Observed Number	Chi-squared Statistic
1	-1.392	35	35	0.000
2	-1.273	35	45	2.857
3	-1.171	35	36	0.029
4	-1.052	35	25	2.857
5	Infinity	35	34	0.029
		175	175	5.771

Notes:

Mean = -1.222

Std Dev = 0.202

Critical Value for Chi-squared = 5.99  
Five structures failed before inspection.

The overall sample of 180 aircraft showed the same characteristics as each of the samples which were based on a single stress level. Therefore, the shape of the distribution does not depend on stress level. All distributions of structural life were confirmed to be normal, and all distributions of inspection crack lengths were confirmed to be lognormal.

After determining the shape of distributions for life and crack length, the deterministic baseline curve shown in Figure 8 was replaced by a stochastic curve, shown schematically in Figure 17.

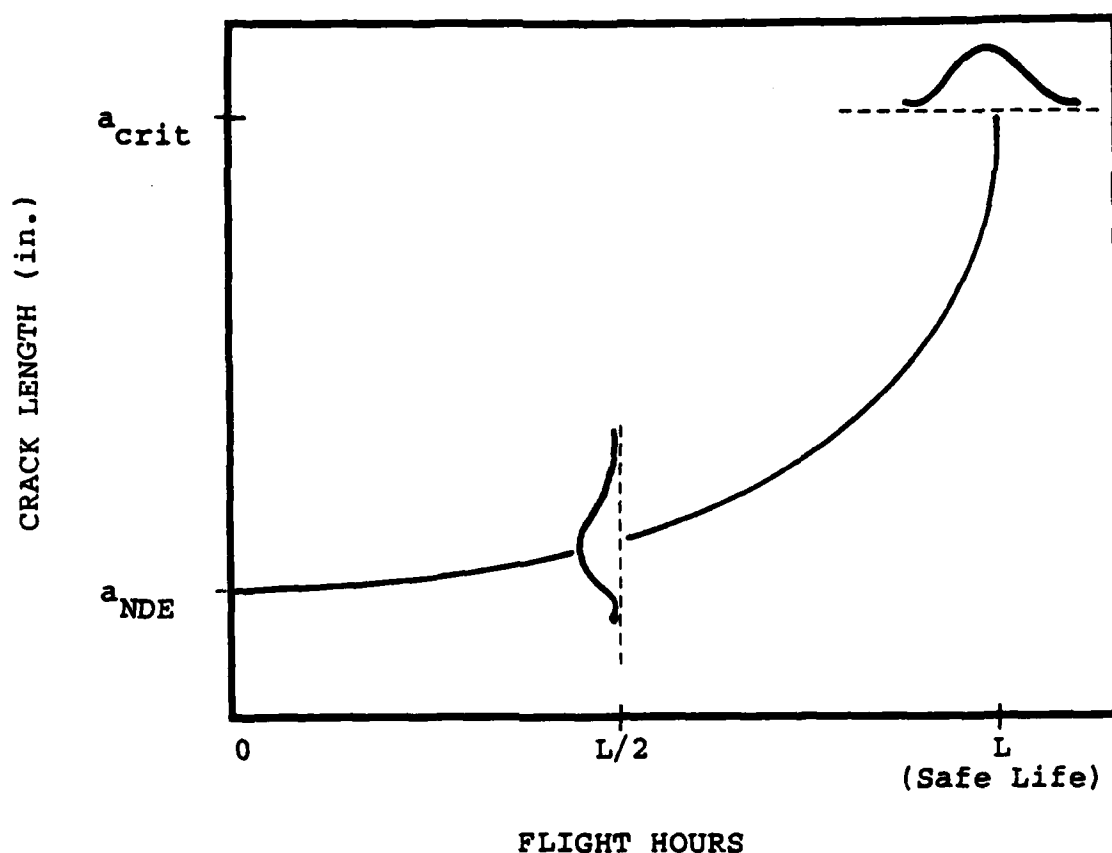


Figure 17. Schematic of Stochastic Crack Growth Curve

Structural Lives. The overall distribution of simulated structural lives was normally distributed with a mean of 4763.82 flight hours and a standard deviation of 1432.12 hours. Using the T test statistic, a 95 percent confidence interval for the mean structural life was determined to be

$$95\% \text{ C.I.} = \bar{X} \pm t_{\alpha/2} \left( \frac{s}{n^{1/2}} \right) \quad (5)$$

where

$\bar{X}$  = Average life  
 $s$  = Sample standard deviation  
 $\alpha$  = Level of Significance

Equation 5 resulted in confidence bounds of approximately 4555 and 4973 flight hours. Thus under similar circumstances, the true mean for all aircraft should fall between these limits 95 percent of the time.

Fleet managers need different information. Decisions concerning maintenance actions deal with the potential failure of individual structures rather than average lives. Therefore, the probability of an structural failure before inspection was assessed. Simulated aircraft lives were normally distributed, so characteristics of the normal probability function were used to determine probable failure rates.

For the standard normal distribution, certain probabilities are associated with each standard deviation

from the mean. For example, 68.27 percent of all values lie within plus or minus one standard deviation of the mean, while 95.45 and 99.73 percent of all values lie within plus or minus two and three standard deviations, respectively (21:A20-A23). The normal distribution is symmetric, so the "two-tailed" approach just described reflects the probability that a value is neither greater than the value associated with Z standard deviations below the mean nor less than the value associated with Z standard deviations above the mean. In determining the probability of structural failures, values above the mean are not relevant and the upper tail (one-half of the difference between 100 percent and the probabilities listed above) is added back in. The probability that a value from the standardized normal distribution will be strictly greater than the value lying Z standard deviations below the mean is shown in Table 19.

Table 19: Probabilities Associated with the Standard Normal Distribution

Number of Standard Deviations From Mean (Z)	Probability that a Value from the Standard Normal Distribution Lies Above Z	
-1	0.8413	(84.13 percent)
-2	0.9773	(97.73 percent)
-3	0.9987	(99.87 percent)

Having defined relevant probabilities, the values for structural life were standardized to fit the standard normal distribution.

$$Z = \frac{X - \bar{X}}{s} \quad (6)$$

where

- Z = The standardized normal random variable  
(Number of standard deviations from mean)
- $\bar{X}$  = The mean value for structural life
- X = A single value for structural life
- s = The sample standard deviation

Using the above information, the probability of a structural failure can be determined for any inspection interval, or the inspection interval can be determined based on any level of risk. Typical results are shown in Tables 20 and 21.

Table 20: Probability of Structural Failure

Inspection Interval (Flight Hours)	Z Value	Probability of Failure (Percent)
2000	-1.930	2.68
2200	-1.790	3.67
2350	-1.685	4.60

Notes:

Based on a mean of 4763.82  
and a standard deviation of 1432.12

Table 21: Required Inspection Intervals

Acceptable Risk of Failure (Percent)	Z Value	Required Inspection Interval (Flight Hours)
1.0	-2.333	1423
2.0	-2.054	1822
5.0	-1.645	2408

Notes:

Based on a mean of 4763.82  
and a standard deviation of 1432.12

Inspection Crack Lengths. Two problems are associated with the structural crack lengths present at the depot-level inspection. First, only cracks below a certain length may be repaired or removed (e.g. by patching or by drilling an oversize hole) to avoid replacing an entire structural component. It is therefore expensive to allow cracks to approach failure, even if the aircraft is not lost. Second, very small cracks are difficult to detect, and the personnel conducting nondestructive inspections may become careless or demotivated if cracks are rarely found. Needless inspections are also very costly. Moreover, some sites can only be inspected after fasteners are removed. Inspecting too often can lead to more damage from fastener removal and replacement than would have resulted with no inspections at all.

The ideal inspection would occur when most structural cracks were detectable with current nondestructive evaluation (NDE) capabilities, and few cracks were longer than the economical repair size. These two criteria were treated separately, since the probability of a crack being outside of the region of interest is simply the sum of the two individual probabilities -- too short to find, and too long to fix.

Proceeding as before, the mean crack length for the 175 aircraft that reached inspection was 0.301 inches, and the standard deviation was 0.066 inches. Based on Equation 5, the 95 percent confidence interval for the mean value is bounded by 0.291 inches and 0.311 inches. Thus, the true mean crack length for all aircraft should fall between these values 95 percent of the time.

To address the problem of repairable crack sizes, the fleet manager would be concerned with Z values of the standard normal distribution above the mean. For the problem of undetectable cracks, he would be concerned with values below the mean. If the mean crack size were within either of the problem areas, then the inspection interval would probably be incorrect. Note that since the distribution of crack lengths was lognormal, all values used in Equation 6 to compute Z were based on the natural log of crack length.

Detectable and repairable crack sizes are set by current capability and cannot be controlled by the fleet manager. The reason for evaluating the distribution of crack sizes is to help determine the most economical inspection technique, and to prevent unnecessary inspections when no cracks are likely to be discovered. The manager determines the degree of risk he is willing to take with respect to needless inspections and costly part replacement. Such a risk analysis is recommended by the Handbook of Force Management Methods.

Experience with the maintenance of existing aircraft has shown that structural problems are relatively minor in comparison to other major aircraft systems. These other systems will tend to drive the scheduling of maintenance activities as they will receive higher priorities. The FSMP [Force Structural Maintenance Plan] should recognize this fact and make allowances for the possibility of subordinating the structural inspection schedule to that of other systems. A risk analysis should be performed to demonstrate any trade-offs that might result from the subordinated schedule. (4: Sec 4,8)

The minimum detectable crack size ( $a_{NDE}$ ) depends on a number of factors, so several arbitrary values were selected to demonstrate the technique. The values are not important. The relative outputs of any two IAT systems can easily be compared so long as the scenario is the same for each. Typical results are shown in Table 22. Values for repairable crack sizes can be evaluated in the same way.

However, since many factors which influence repairable crack size were not addressed in this simulation, probabilities were not assigned to repairable cracks.

Table 22: Probability of Undetectable Crack Sizes

Crack Size (a)	Z Value	Probability of Occurrence
Less than 0.1500 in	-3.340	0.04 percent
Less than 0.1875 in	-2.238	1.26 percent
Less than 0.2000 in	-1.918	2.76 percent
Less than 0.2250 in	-1.335	9.09 percent
Less than 0.2500 in	-0.813	20.71 percent

Notes:

Based on a normal distribution of  $\ln(a)$   
Mean = -1.222      Standard Deviation = 0.202

Summary of Results

Structural lives were normally distributed with a mean 4763.82 flight hours and a standard deviation of 1432.12 hours. Using these values, along with characteristics of the standard normal distribution, required inspection intervals were determined based on selected levels of risk. The risk associated with selected inspection intervals was also evaluated. Results were for a single IAT system. Various IAT systems could be directly compared with one another by using a common scenario and assessing relative inspection requirements and risks.

The lengths of structural cracks found at the one-half lifetime depot inspection were lognormally distributed. The mean crack length ( $a$ ) was 0.301 inches with a standard deviation of 0.066 inches. To simplify analysis, data were expressed as a normal distribution of  $\ln(a)$  with a mean of -1.222 and a standard deviation of 0.202. The probability that a crack was either too small to detect or too large to repair was calculated at the one-half lifetime inspection. Information on what to expect allows managers to plan more effectively, and to devote appropriate resources. It can also help them determine which NDE techniques are appropriate based on required accuracy.

## V. Discussion

Chapter IV presented the results of the overall simulation. This chapter evaluates those results in terms of the simulation inputs. By understanding the effects and relative importance of various parameters on the IAT analyses, future simulations can provide more specific answers with less resources.

### Material Properties

Naturally occurring differences in material properties had a significant effect on simulation outcomes. With all other parameters held constant, the average structural lives ranged from 3103.80 flight hours to 6483.57 flight hours. Each average was calculated based on a single set of material constants, and included 15 data points. Expressed in terms of the overall simulation, the range was 65 percent to 136 percent of the mean.

Results were similar for the simulated inspection crack lengths. The average crack length ranged from 0.246 inches to 0.399 inches (82% to 133% of the mean). However, since some structures failed before reaching inspection, all samples did not have the same number of data points.

Summary information is provided in Table 23. Although material constants cannot be controlled by the IAT process, their effects on structural behavior are extremely important to any simulation involving an IAT system.

Table 23: Summary of Simulation Results by Material Constants

CONSTANTS			LIFE			INSPECTION CRACK LENGTH		
#	C	N	Mean (Flt Hrs)	Standard Deviation	No. of Points	Mean (Inches)	Standard Deviation	No. of Points
6	1.984E-8	2.234	6483.57	1210.57	15	0.246	0.021	15
8	1.105E-8	2.446	6083.63	1240.04	15	0.250	0.025	15
4	1.136E-8	2.448	5853.67	1192.56	15	0.256	0.026	15
2	8.204E-9	2.594	5123.78	1085.69	15	0.278	0.035	15
10	7.462E-9	2.608	5443.73	1119.99	15	0.266	0.032	15
3	7.991E-9	2.627	4713.85	1021.08	15	0.296	0.042	15
12	6.462E-9	2.705	4553.88	991.58	15	0.302	0.047	15
5	5.597E-9	2.784	4083.95	916.53	15	0.333	0.062	15
1	3.727E-9	2.891	4433.90	1051.70	15	0.305	0.054	15
7	3.607E-9	2.961	3604.03	844.76	15	0.360	0.067	14
9	2.653E-9	3.053	3684.02	898.42	15	0.349	0.066	14
11	1.545E-9	3.275	3103.80	790.71	15	0.399	0.086	12
All Tests								
7.458E-9	2.719		4763.82	1432.12	180	0.301	0.066	175
Expected								
7.403E-9	2.631		4696.82	-----	1	0.282	-----	1

Notes:

Five structures failed before the scheduled inspection.

Entries were sorted according the Walker slope, N.

The "#" column indicates the order used in other tables.

A Tukey range test (9:355-357) was conducted to determine which sets of material constants produced statistically equivalent results. The level of significance for the multiple comparison was 0.05, resulting in a simultaneous confidence level of 95 percent. Tables 24 and 25 show groups of material constants that produced statistically similar results. Set numbers refer to the "#" index used in Table 23.

Table 24: Groups of Material Constants that Produced Statistically Similar Structural Lives

Group	Similar Sets of Material Constants
A	6,8,4,10
B	8,4,10,2
C	4,10,2,3
D	10,2,3,12,1
E	2,3,12,1,5
F	3,12,1,5,9,7
G	5,9,7,11

Table 25: Groups of Material Constants that Produced Statistically Similar Inspection Crack Lengths

Group	Similar Sets of Material Constants
A	6,8,4,10,2,3,12,1
B	2,3,12,1,5
C	3,12,1,5,9
D	12,1,5,9,7
E	9,7,11

The relationship between the slope of the crack growth rate curve and the resulting structural life should be very strong. Therefore, the relationship was evaluated to determine if it was linear. For each of the five load histories at each of the three stress levels, the twelve values for the Walker slope  $N$  were plotted against corresponding structural lives. Individual least squares linear regressions for the 15 plots resulted in coefficients of determination ( $r^2$ ) that were all between 0.90 and 0.94. Thus, the relationship was considered to be linear. For a given stress level, knowing the Walker slope allowed a reasonable estimate of the structural life. This relationship must be coupled with the stress intensity factor,  $\Delta K$ , before it has meaning for other simulations or experiments, but it worked very well for a specific structural geometry and initial crack length.

#### Load History Variations

All load history variations used in this study were based on the same exceedance curve and theoretically should have produced identical results (18). However, average simulated structural lives ranged from 3863.95 flight hours to 5873.92 flight hours when other parameters were held constant. This range was from 81 percent to 123 percent of the overall mean. Average crack lengths at inspection ranged from 0.257 inches to 0.345 inches (85% to 115% of the overall mean). Summary information is provided in Table 26.

Table 26: Summary of Simulation Results by Load History

LOAD HISTORY	LIFE			INSPECTION CRACK LENGTH		
	Mean (Flt Hrs)	Standard Deviation	No. of Points	Mean (Inches)	Standard Deviation	No. of Points
Baseline	4534.35	1260.08	36	0.309	0.061	35
RF2	3863.95	1150.25	36	0.345	0.072	32
RMP1F	4651.49	1254.70	36	0.308	0.071	36
RMP1	4895.39	1278.88	36	0.291	0.055	36
RMP2	5873.92	1477.54	36	0.257	0.038	36
All Tests	4763.82	1432.12	180	0.301	0.066	175
Expected	4696.82	-----	1	0.282	-----	1

Notes:

Five structures failed before the scheduled inspection.

Too few load history variations were used to allow definitive conclusions on the relative merits of the reconstitution algorithms. However, the two variations developed using 0.2 g increments (RF2 and RMP2) produced significantly different results from the variations developed using 0.1 g increments, and from the overall mean. Therefore, the sensitivity of the IAT recorder appears to have an important influence on life predictions. The magnitude of that influence cannot be determined without further study.

The cycle-by-cycle and flight-by-flight variations (RMP1 and RMP1F) produced results that were consistently about five percent apart. In a simulation of this complexity, that difference is negligible. The similarity between results for RMP1 and RMP1F confirm the opinion of Reference 18 that the sequence of flight loads is not crucial to the reconstitution of a load history, so long as a single repetition of the load history comprises less than five percent of the total aircraft life. Since the load histories used in this study represented 150 flight hours, they comprised only about three to five percent of a lifetime.

Based on the Tukey range test, load histories RMP1 and RF2 produced significantly different lives when compared with one another. Load history RMP2 produced lives significantly different from all other load histories.

All other combinations of average lives were statistically similar. Inspection crack lengths were not evaluated with the Tukey range test.

### Stress Levels

The three stress levels evaluated represented the stresses due to expected aircraft gross weight, and variations of plus and minus five percent. Average results are shown in Table 27. A five percent increase in stress level led to approximately a 21 percent increase in structural life. Conversely, a five percent decrease in stress led to approximately an 18 percent decrease in life.

The effects of stress level on structural life observed during this study were linear. In fact, for every load history, the three points for average life vs stress level fell along a straight line. Three points per load history are hardly enough to justify firm conclusions, but the consistency of the relationship for all five load histories indicates that the effects of stress level could be predicted. Quantifying that relationship would greatly reduce the resources required for future simulations.

### Combined Effects

Since structural lives were linearly related to both the Walker slope ( $N$ ) and the stress level ( $\sigma$ ), a multiple regression was conducted for life as a function of  $N$  and  $\sigma$ .

Table 27: Summary of Simulation Results by Stress Level

MAXIMUM STRESS	LIFE			INSPECTION CRACK LENGTH		
	Mean (Flt Hrs)	Standard Deviation	No. of Points	Mean (Inches)	Standard Deviation	No. of Points
38 ksi	5703.69	1413.64	60	0.271	0.050	60
40 ksi	4703.78	1210.90	60	0.302	0.061	59
42 ksi	3883.99	1033.70	60	0.333	0.071	56
All Tests	4763.82	1432.12	180	0.301	0.066	175
Expected	4696.82	-----	1	0.282	-----	1

Notes:

Five structures failed before the scheduled inspection.

The regression produced an equation for life,

$$L = 32485 - 455\sigma - 3503N \quad (7)$$

where

L = Structural life (flight hours)  
 $\sigma$  = Maximum stress (ksi)  
N = Walker slope

The multiple  $r^2$  for the regression was 0.94.

Equation 7 provided very good predictions of simulation results for each stress level. The data being predicted were the same data used to generate the equation, and were based on a single geometry and fixed initial crack length. Consequently, the results do not indicate a generic predictive capability. The equation will not be applicable to other data until initial and final values for the stress intensity factor,  $\Delta K$ , are incorporated into the regression. Nevertheless, the success of the predictions confirms that there is a strong quantifiable relationship between the Walker slope, the stress level, and structural life. A comparison of predicted and simulated structural lives is provided in Table 28.

If the stress intensity factor were incorporated into the regression, Equation 7 could be transformed into a general formula for structural life. Such a formula would reduce simulation resource requirements by several orders of magnitude. Developing the formula requires additional data

### Table 28: Comparison of Simulated and Predicted Lives

WALKER SLOPE (N)	38 ksi		40 ksi		42 ksi				
	Predicted	Simulated Ratio	Predicted	Simulated Ratio	Predicted	Simulated Ratio			
2.891	5067.83	5403.74	0.94	4157.83	4353.91	0.95	3247.83	3544.04	0.92
2.594	6108.22	6123.62	1.00	5198.22	5073.79	1.02	4288.22	4173.94	1.03
2.627	5992.62	5643.70	1.06	5082.62	4653.86	1.09	4172.62	3843.99	1.09
2.448	6619.66	6963.49	0.95	5709.66	5793.68	0.99	4799.66	4803.84	1.00
2.784	5442.65	4923.82	1.11	4532.65	4023.96	1.13	3622.65	3304.08	1.10
2.234	7369.30	7623.38	0.97	6459.30	6423.58	1.01	5549.30	5403.74	1.03
2.961	4822.62	4353.91	1.11	3912.62	3544.04	1.10	3002.62	2914.14	1.03
2.446	6626.66	7263.44	0.91	5716.66	6003.64	0.95	4806.66	4983.81	0.96
3.053	4500.34	4473.89	1.01	3590.34	3604.03	1.00	2680.34	2974.13	0.90
2.608	6059.18	6483.57	0.93	5149.18	5373.75	0.96	4239.18	4473.89	0.95
3.275	3722.68	3754.01	0.99	2812.67	3063.18	0.92	1902.67	2494.21	0.76
2.705	5719.39	5433.74	1.05	4809.39	4533.88	1.06	3899.39	3694.02	1.06
Mean: 2.719	5670.93	5703.69	1.00	4760.93	4703.78	1.01	3850.93	3883.99	0.99

**Notes:**

**Predictions were made based on the equation**

$$\text{Life} = 32485 - 455 * (\text{Stress}) - 3503 * (\text{slope})$$

where stress is in ksi, and life is in flight hours.

**Each simulated life is the average for five load histories.**

analysis that was beyond the scope of this thesis, but some supporting information is provided in Appendix C.

### Summary

Inputs to the simulation were material properties, load histories, and maximum stress levels. Several values were chosen for each of these three variables, representing typical variations (errors) encountered in the IAT program.

By examining the effects of one variable at a time with the others held constant, it was determined that naturally occurring differences in "identical" pieces of structural material led to lives which were as much as 35 percent above or below the sample mean. Differences in "identical" load histories led to deviations of approximately 20 percent above and below the mean. The difference in load histories appeared to be due to recorder sensitivity rather than the sequence of flight loads within the history. Finally, a five percent error in the assumed stress level of the load history also led to approximately a 20 percent deviation above and below the mean.

The relationship for structural life as a function of the Walker slope ( $N$ ) and stress level ( $\sigma$ ) was linear for the structural geometry studied in this simulation. If this relationship were expanded to include initial and final values for the stress intensity factor ( $\Delta K$ ), a formula could be developed which would reduce future simulation resource requirements by several orders of magnitude.

## VI. Conclusions and Recommendations

### Conclusions

The technique demonstrated in this thesis shows great promise for providing meaningful comparisons of various IAT systems. By selecting a realistic scenario and conducting the same simulation for several IAT devices and data reduction techniques, the strengths and weaknesses of each system can be evaluated. These strengths and weaknesses can then be used to determine appropriate safety factors for each individual IAT system, and to specify areas of emphasis for developing future IAT systems.

Using procedures demonstrated in this report, a manager can determine the probability of structural failure within a fleet of aircraft based on any specified inspection interval. He can also determine the inspection interval required to maintain a specified level of risk. This capability gives him concrete tools to help evaluate the impact of changing maintenance schedules on aircraft safety.

Material crack growth properties based on the Walker equation were easily simulated using normal and lognormal distributions. Naturally occurring variations in material properties had a significant effect on structural life. The material evaluated in this study came from a single production lot of 2024-T3 aluminum. Although the simulation needs to be expanded to include several lots of material, it

is unlikely that the shape of the underlying distributions will change significantly.

The effects of load history variations on structural life were also significant. The sequence of flight loads did not appear to be important, but the sensitivity of the flight loads recorder had a major impact on simulated lives. The five load history variations used in this study were all based on the same exceedance curve. Average lives for these variations differed by as much as 50 percent.

Only three stress levels were evaluated, so no firm conclusions were possible concerning the relationship between stress level and structural life. However, for every load history variation, the three points for average life vs stress fell along a straight line. The consistency of these results indicates that the effects of stress level could be predicted.

A regression equation was developed for structural life as a function of stress and the Walker slope  $N$ . The equation provided excellent predictions of lives for all load history variations. If initial and final values for the stress intensity factor were incorporated into the regression, a general formula for structural life might be possible. Such a formula would reduce simulation resource requirements by several orders of magnitude.

## Recommendations

The simulation described in this thesis should be expanded to include the data capture rates typical of selected IAT devices. In addition, a distribution of initial flaw sizes should be used in lieu of a single fixed crack size. For a direct comparison of IAT systems, a reasonable estimate of the crack size distribution would suffice. In that way, the probabilities of structural failure would more closely approximate real world percentages.

Several years of extensive data collection and analysis are still required before the initial flaw distributions can be modeled well enough to allow a truly stochastic approach to IAT. However, the approach outlined in this thesis is sufficient to provide valuable information concerning relative strengths and weaknesses of IAT systems. It is highly recommended that current and planned IAT systems be evaluated using such an approach. Individual system safety factors should then be developed. It simply does not make sense to apply the same safety factor to IAT systems developed with 1980's technology as is applied to systems from the 1950's. The collection of more and better information should be reflected by increased confidence in the system.

To reduce the resource requirements of future simulations, the relationship between stress levels,

AD-A160 146

PROBABILISTIC EVALUATION OF INDIVIDUAL AIRCRAFT

2/2

TRACKING TECHNIQUES(U) AIR FORCE INST OF TECH

WRIGHT-PATTERSON AFB OH SCHOOL OF SYST.

**R L WILKINSON**

UNCLASSIFIED

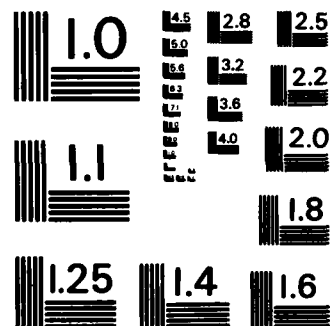
SEP 85 AFIT/GSM/ENS/855-32

F/G 1/3

ML

END

Q144.



MICROCOPY RESOLUTION TEST CHART  
NATIONAL BUREAU OF STANDARDS - 1963 - A

material constants, and structural geometries should be fully explored. The formula developed for structural life in terms of the Walker slope (N) and structural stress level ( $\sigma$ ) should be expanded to include initial and final values for the stress intensity factor ( $\Delta K$ ). Such a formula has the potential to drastically reduce the time and resources required for structural life calculations of all types.

Finally, the material properties data examined in this report should be expanded to represent expected fleet-wide variability. The present data is sufficient for the comparison of IAT systems, but much more information is required before a transition to stochastic IAT can successfully take place.

## Appendix A: Material Properties Simulation

The simulation discussed in Chapter III is only as valid as its input data. Obtaining realistic values for input variables was extremely important. Therefore, data from Reference 29 were analyzed in a separate simulation to determine the expected variation in material properties for aluminum alloys. The tests were conducted at Purdue University using identical center-cracked panels of 2024-T3 aluminum. All panels were six inches wide by 0.10 inches thick and experienced constant amplitude loading at a maximum stress of 8.75 ksi, based on gross section area. The stress ratio (R) was 0.20.

Each of the 68 replicate tests provided 164 data points representing an individual crack growth curve. To make the data useful for analysis, the derivative of each curve was calculated using the modified secant method.

$$\left( \frac{da}{dn} \right)_i = \frac{\frac{a_{i+1} - a_i}{n_{i+1} - n_i} + \frac{a_i - a_{i-1}}{n_i - n_{i-1}}}{2} \quad (A1)$$

where

a = Half crack length  
n = Cycle count  
i = Current data point

$\frac{da}{dn}$  = Crack growth rate

Data were then plotted against the stress intensity factor,  $\Delta K$ , which is a standard geometric correction factor used to allow comparison of data from varying test conditions. The equation for  $\Delta K$  is

$$\Delta K = \Delta \sigma \sqrt{\pi a} \beta \quad (A2)$$

where

$$\beta = 1 + 0.256(a/w) - 1.152(a/w)^2 + 12.19(a/w)^3$$

$w$  = Specimen width (inches)

$\Delta \sigma$  = Delta stress (ksi)

$a$  = Half crack length (inches)

Figure A1 shows the plot of crack growth rate vs stress intensity factor for the linear range ( $9 < \Delta K < 18$ ) of data. The range of selected  $\Delta K$  values is appropriate for this simulation because the combination of initial crack length and stress level used for computations ensured that the stress intensity factor would never fall significantly below the linear region. Moreover, the majority of a specimen's total cyclic life is accounted for by the lower regions of the  $da/dn$  vs  $\Delta K$  curve (23:83). Therefore, the choice of final crack length, should it be above the linear range of  $\Delta K$  values, has a very minor impact on total specimen life. The actual range of  $\Delta K$  values used for the material properties simulation in Appendix A was  $8.87 < \Delta K < 17.55$ .

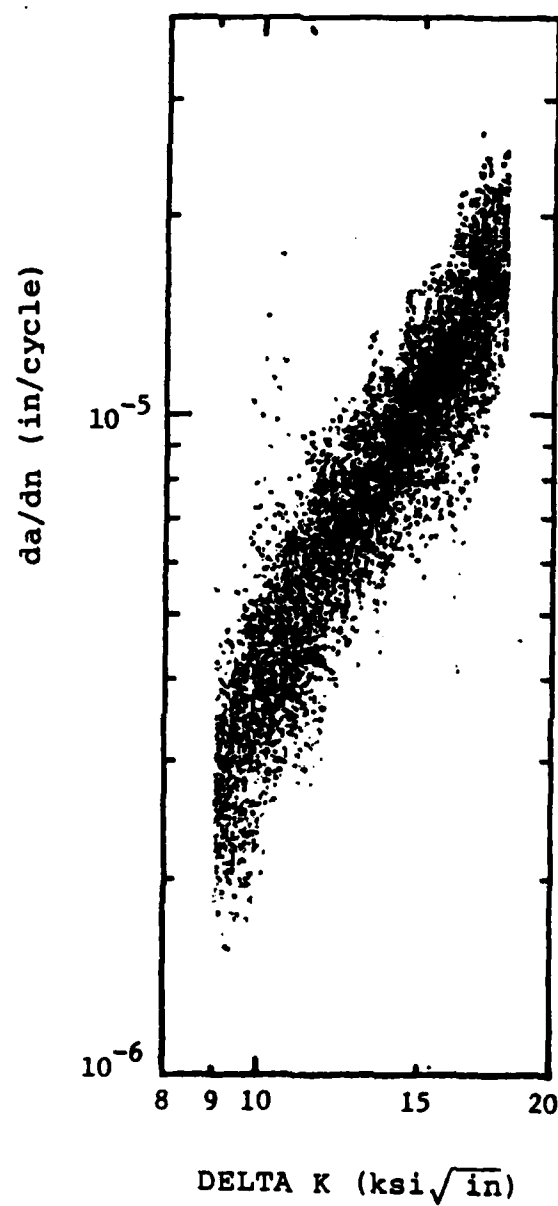


Figure A1. Crack Growth Rate Curves (68 Curves, 8228 Points)

Using a standard least squares linear regression (Paris fit), the above data were curve-fit to obtain the equations for 68 straight lines in log-log space.

$$\left(\frac{da}{dn}\right)_i = b_0 \Delta K_i^{b_1} \quad (A3)$$

However, the CRACKS4 analysis required a Walker equation,

$$\left(\frac{da}{dn}\right)_i = C \left[ \Delta K_i (1-R)^{m-1} \right]^N \quad (A4)$$

where

$$R = \text{Stress Ratio}$$

Since the number of unknowns in Equations A3 and A4 is not compatible, the Walker value for "m" was fixed. This is acceptable because m is a collapsing factor used to account for the effects of differing stress ratios. Only one stress ratio was used to generate the data under analysis. Thus, Equation A4 can be expressed as

$$\left(\frac{da}{dn}\right)_i = C \left[ ((1-R)^{m-1})^N \right] \Delta K_i^N \quad (A5)$$

Solving for C and N in terms of Equation A3:

$$C = \frac{b_0}{\left[ (1-R)^{m-1} \right]^N} \quad (A6)$$

$$N = b_1 \quad (A7)$$

For the Purdue test data, the stress ratio (R) was 0.2. The fixed value of  $m=0.682$  was obtained from Reference 19. Values for  $b_0$ ,  $b_1$ , and  $r^2$  for all least squares fits, along with calculated values for the Walker constants C and N, are listed in Table A2. Summary information is provided in Table A1. The reason for calculating  $\ln(C)$  will be explained later.

Table A1: Summary of Curve-Fit Results\*

Quantity	Mean	Standard Deviation
N	2.620	0.275
C	$1.010 \times 10^{-9}$	$1.023 \times 10^{-8}$
$\ln(C)$	-18.694	0.685

\*Notes:

Standard deviations were calculated from the following equation for variance (9:88),

$$s^2 = E(X^2) - [E(X)]^2$$

which is equivalent to

$$s^2 = \frac{\sum (X_i - \bar{X})^2}{n}$$

Table A2: Curve-Fit Results

RESULTS OF CURVE-FITTING (121 Points per Test) Walker Constant m=0.682, Stress Ratio=0.2					
TEST	LEAST SQUARES			WALKER EQ.	
	SLOPE	INTERCEPT	$r^2$	C	N
1	2.666	8.422E-09	0.916	6.970E-09	2.666
2	2.754	6.779E-09	0.924	5.575E-09	2.754
3	2.900	4.995E-09	0.879	4.066E-09	2.900
4	2.885	4.856E-09	0.908	3.957E-09	2.885
5	2.795	6.031E-09	0.921	4.946E-09	2.795
6	2.654	8.835E-09	0.939	7.319E-09	2.654
7	2.800	6.318E-09	0.927	5.180E-09	2.800
8	2.830	5.628E-09	0.951	4.604E-09	2.830
9	3.008	3.834E-09	0.797	3.097E-09	3.008
10	3.013	3.386E-09	0.931	2.734E-09	3.013
11	2.940	3.961E-09	0.942	3.216E-09	2.940
12	3.015	3.662E-09	0.939	2.957E-09	3.015
13	2.586	1.070E-08	0.889	8.908E-09	2.586
14	2.803	5.987E-09	0.902	4.907E-09	2.803
15	2.947	4.787E-09	0.908	3.884E-09	2.947
16	2.696	7.526E-09	0.936	6.216E-09	2.696
17	2.657	8.393E-09	0.943	6.951E-09	2.657
18	2.837	5.263E-09	0.899	4.303E-09	2.837
19	2.642	8.466E-09	0.912	7.019E-09	2.642
20	2.672	8.096E-09	0.885	6.697E-09	2.672
21	2.289	2.012E-08	0.918	1.710E-08	2.289
22	2.521	1.164E-08	0.864	9.731E-09	2.521
23	2.346	1.902E-08	0.927	1.610E-08	2.346
24	2.671	7.341E-09	0.928	6.074E-09	2.671
25	2.163	2.843E-08	0.850	2.439E-08	2.163
26	2.333	1.832E-08	0.814	1.552E-08	2.333
27	2.390	1.666E-08	0.768	1.406E-08	2.390
28	1.926	5.066E-08	0.745	4.419E-08	1.926
29	2.678	7.708E-09	0.949	6.374E-09	2.678
30	2.546	1.114E-08	0.885	9.298E-09	2.546
31	2.741	7.098E-09	0.800	5.844E-09	2.741
32	3.011	3.500E-09	0.932	2.827E-09	3.011
33	2.505	1.243E-08	0.941	1.041E-08	2.505
34	2.708	7.471E-09	0.885	6.165E-09	2.708

Table A2 (Continued)

RESULTS OF CURVE-FITTING (121 Points per Test) Walker Constant m=0.682, Stress Ratio=0.2					
TEST	LEAST SQUARES			WALKER EQ.	
	SLOPE	INTERCEPT	$r^2$	C	N
35	2.518	1.080E-08	0.861	9.031E-09	2.518
36	2.341	1.691E-08	0.889	1.433E-08	2.341
37	2.340	1.543E-08	0.769	1.307E-08	2.340
38	2.517	1.289E-08	0.891	1.078E-08	2.517
39	2.559	1.102E-08	0.900	9.190E-09	2.559
40	2.651	8.716E-09	0.871	7.221E-09	2.651
41	2.383	1.713E-08	0.920	1.446E-08	2.383
42	2.741	7.215E-09	0.905	5.940E-09	2.741
43	2.619	8.844E-09	0.902	7.344E-09	2.619
44	2.212	2.144E-08	0.621	1.833E-08	2.212
45	2.620	8.746E-09	0.835	7.262E-09	2.620
46	2.579	8.757E-09	0.825	7.293E-09	2.579
47	1.814	6.640E-08	0.738	5.838E-08	1.814
48	2.569	8.662E-09	0.907	7.218E-09	2.569
49	1.835	5.763E-08	0.511	5.060E-08	1.835
50	2.749	6.503E-09	0.875	5.351E-09	2.749
51	2.616	9.167E-09	0.918	7.615E-09	2.616
52	2.416	1.469E-08	0.899	1.238E-08	2.416
53	2.464	1.365E-08	0.894	1.146E-08	2.464
54	2.831	5.722E-09	0.922	4.681E-09	2.831
55	2.563	1.034E-08	0.928	8.621E-09	2.563
56	3.132	2.504E-09	0.943	2.005E-09	3.132
57	2.694	8.089E-09	0.930	6.681E-09	2.694
58	2.882	4.838E-09	0.940	3.943E-09	2.882
59	2.871	5.335E-09	0.933	4.351E-09	2.871
60	2.954	3.701E-09	0.930	3.001E-09	2.954
61	2.488	1.187E-08	0.889	9.949E-09	2.488
62	2.983	3.904E-09	0.951	3.159E-09	2.983
63	2.405	1.684E-08	0.876	1.420E-08	2.405
64	2.665	8.596E-09	0.912	7.115E-09	2.665
65	2.881	4.288E-09	0.916	3.495E-09	2.881
66	2.579	1.089E-08	0.927	9.072E-09	2.579
67	2.680	3.535E-09	0.896	7.057E-09	2.680
68	2.107	3.564E-08	0.909	3.069E-08	2.107

### Determining the Distributions

The first step in determining the distributions for C and N was to plot histograms. The resulting plots are shown in Figures A2 and A3.

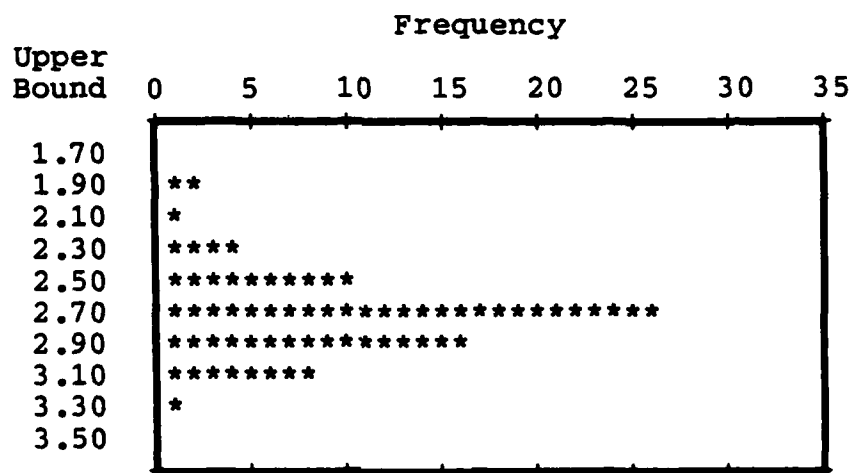


Figure A2. Histogram for Walker Slope N

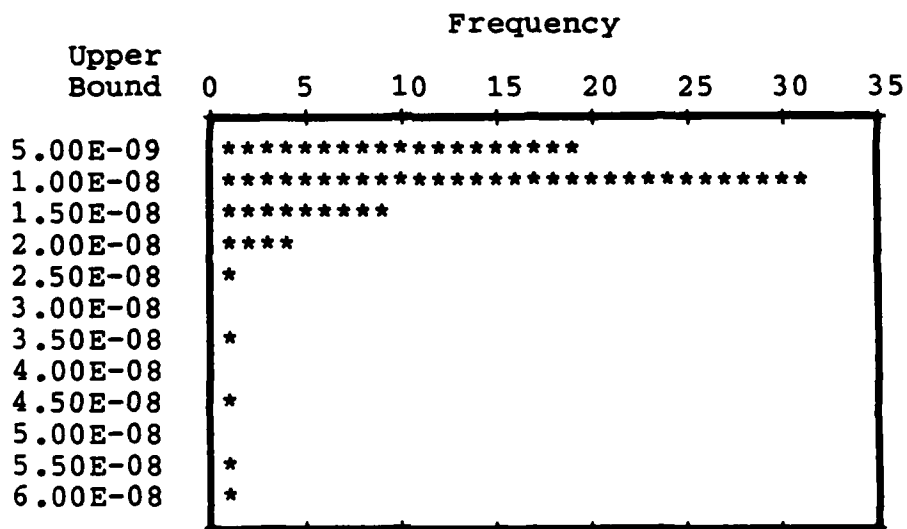


Figure A3. Histogram for Walker Intercept C

The distribution of values for N appeared to follow a Weibull pattern, so that distribution was evaluated. The Weibull parameters were generated using the iterative technique described in Reference 2. The technique involves selecting an initial value for beta,

$$\hat{\beta}_0 = \frac{\bar{X}}{S} \quad (A8)$$

and iterating

$$\hat{\beta}_j = \hat{\beta}_{j-1} - \frac{f(\hat{\beta}_{j-1})}{f'(\hat{\beta}_{j-1})} \quad (A9)$$

where

$$f(\beta) = \frac{n}{\beta} + \sum_{i=1}^n \ln X_i - \frac{n \sum_{i=1}^n X_i^\beta \ln X_i}{\sum_{i=1}^n X_i^\beta} \quad (A10)$$

$$f'(\beta) = \frac{-n}{\beta^2} - \frac{n \sum_{i=1}^n X_i^\beta (\ln X_i)^2}{\sum_{i=1}^n X_i^\beta} + \frac{n \left( \sum_{i=1}^n X_i^\beta \ln X_i \right)^2}{\left( \sum_{i=1}^n X_i^\beta \right)^2} \quad (A11)$$

Once Equation A9 converges so that  $f(\beta) < 0.001$ , then  $\beta$  is used to calculate  $\alpha$  as follows:

$$\alpha = \left( \frac{1}{n} \sum_{i=1}^n X_i^\beta \right)^{1/\beta} \quad (A12)$$

Knowing appropriate values of alpha and beta for the distribution, a goodness of fit test was conducted. Therefore, the Weibull distribution was found to adequately represent the empirical distribution of N values (Table A3).

Table A3: Chi-Squared Fit for Weibull Distribution of N\*

Cell	Upper Bound	Expected Number	Observed Number	Chi-squared Statistic
1	2.263	6.8	6	0.094
2	2.411	6.8	8	0.212
3	2.509	6.8	4	1.153
4	2.586	6.8	10	1.506
5	2.653	6.8	5	0.476
6	2.717	6.8	11	2.594
7	2.780	6.8	4	1.153
8	2.849	6.8	6	0.094
9	2.934	6.8	5	0.476
10	Infinity	6.8	9	0.712
		68.0	68	8.471

\* Notes:

Alpha = 2.7369                      Mean = 2.6204  
Beta = 11.8386                      Std Dev = 0.2745

Level of Significance = 0.05  
Critical Value for Chi-Squared = 14.1

The distribution of values for C appeared to be exponential (Fig. A3), but failed goodness of fit testing for that distribution. Consequently, a lognormal distribution was considered. For simplicity, a goodness of fit test was conducted for a normal distribution of  $\ln(C)$  values. The histogram for  $\ln(C)$  is shown in Figure A4, and the goodness of fit results are shown in Table A4.

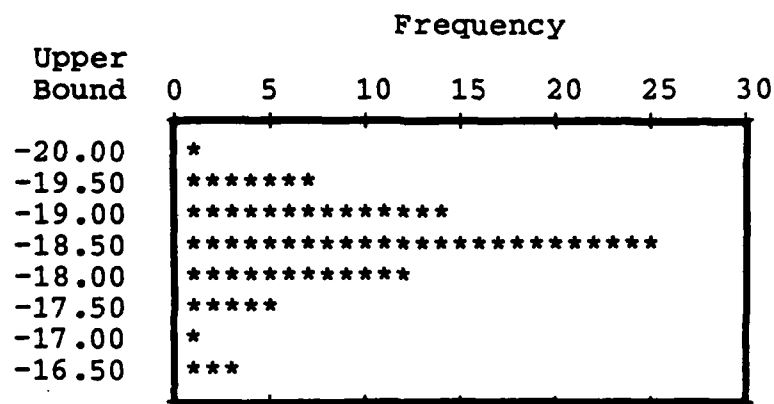


Figure A4. Histogram for Ln(C)

Table A4: Chi-squared fit for Normal Distribution of ln(C) \*

Cell	Upper Bound	Expected Number	Observed Number	Chi-squared Statistic
1	-19.572	6.8	7	0.006
2	-19.270	6.8	6	0.094
3	-19.053	6.8	7	0.006
4	-18.867	6.8	8	0.212
5	-18.694	6.8	13	5.653
6	-18.521	6.8	4	1.153
7	-18.335	6.8	7	0.006
8	-18.117	6.8	3	2.124
9	-17.816	6.8	7	0.006
10	Infinity	6.8	6	0.094
		68.0	68	9.354

\* Notes:

Mean = -18.6938      Std Dev = 0.6848

Level of Significance = 0.05

Critical Value for Chi-Squared = 14.1

Since C followed a lognormal distribution, it became worthwhile to see if the values for N could be represented by a normal distribution, as well as by the Weibull. Based on the histogram shown in Figure A2, the goodness of fit testing for a normal distribution is shown below (Table A5).

Table A5: Chi-Squared fit for a Normal Distribution of N<sup>\*</sup>

Cell	Upper Bound	Expected Number	Observed Number	Chi-squared Statistic
1	2.268	6.8	6	0.094
2	2.389	6.8	6	0.094
3	2.477	6.8	4	1.153
4	2.551	6.8	6	0.094
5	2.620	6.8	8	0.212
6	2.690	6.8	11	2.594
7	2.764	6.8	7	0.005
8	2.852	6.8	6	0.094
9	2.972	6.8	7	0.005
10	Infinity	6.8	7	0.005
		68.0	68	4.350

\* Notes:

Mean = 2.6204                      Std Dev = 0.274513

Level of Significance = 0.05

Critical Value for Chi-Squared = 14.1

The values for N passed tests for both distributions, so the probability density functions were plotted over the histogram to see if there appeared to be any significant advantage to using the Weibull distribution. As is shown in Figure A5, and confirmed by the goodness of fit tests, both approaches provide a reasonable fit of the data.

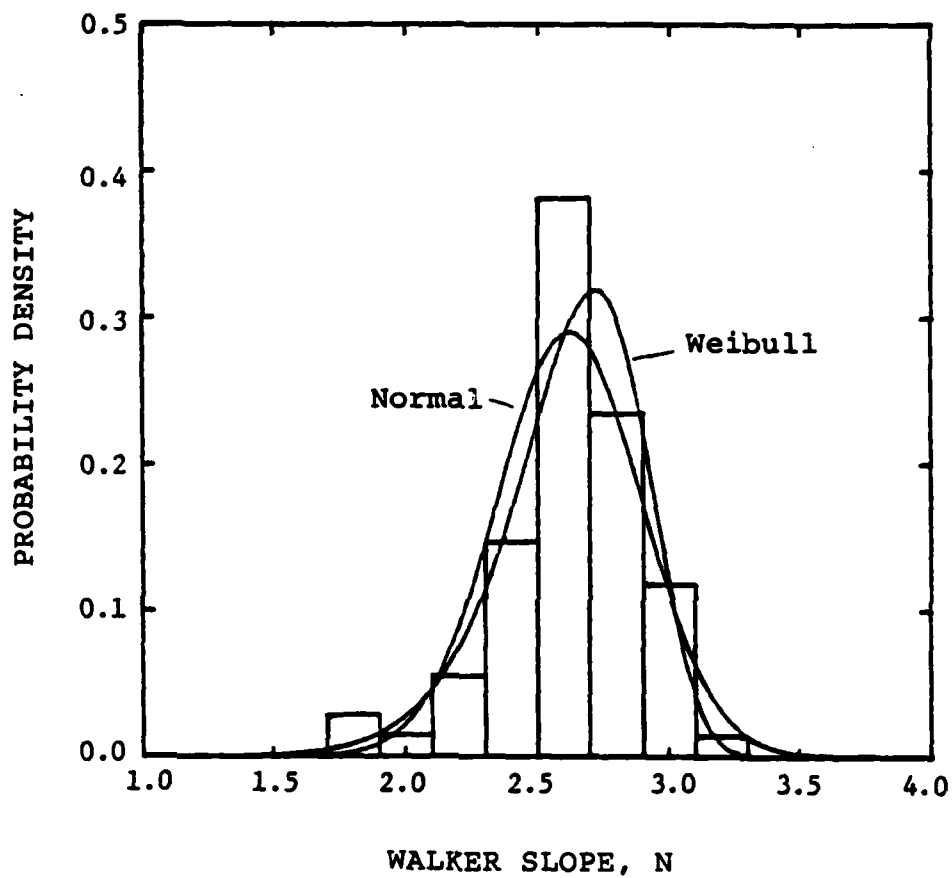


Figure A5. Probability Density Functions Overlaid on Histogram for  $N$

## Testing the Random Number Generator

Random variates for use in the material properties simulation were generated using the "MBASIC" RND(1) function on a Pertec PCC 2000 microcomputer. Since personal computers have a poor reputation for generating acceptable pseudorandom numbers, an analysis of the random number stream was conducted. Tables A6 through A8 summarize the tests for uniformity and independence. Each random number stream consisted of 100 integers between 0 and 99 inclusive.

The random number generator passed both the Chi-square test for uniformity and the Runs Above and Below the Mean test for independence for each of the number streams generated. Therefore, the RND(1) function was used to generate all random numbers for the simulation.

Table A6: Runs Above and Below the Mean<sup>\*</sup>  
Test for Independence

Trial	Mean	Var.	Total Runs	Runs Mean	Above Mean	Below Mean	Z Value
1	49.25	1018.3	58	50.5	50	50	1.51
2	44.53	838.6	57	50.5	49	51	1.31
3	51.04	818.8	47	50.2	54	46	-0.64
4	48.50	916.0	55	50.3	47	53	0.94
5	49.67	910.1	57	50.2	54	46	1.38

<sup>\*</sup> Notes:

Each trial consisted of 100 integers between 0 and 100.  
Expected values were -- Mean: 50.0, Variance: 833.33  
Level of Significance = 0.05  
Critical Values for Z and T: +1.96  
All values were obtained from Reference 10.  
Formulas were taken from Reference 2.

Table A7: Chi-squared Test for Uniformity --  
Observed Values

Cell	Range	Run 1	Run 2	Run 3	Run 4	Run 5
1	[ 0,10)	15	16	11	12	9
2	[10,20)	7	7	7	11	16
3	[20,30)	12	11	10	9	9
4	[30,40)	8	12	9	11	8
5	[40,50)	8	10	7	11	4
6	[50,60)	8	11	12	4	10
7	[60,70)	5	11	11	11	11
8	[70,80)	13	5	16	7	12
9	[80,90)	14	8	8	13	9
10	[90,100)	10	9	9	11	12

Table A8: Chi-squared Test for Uniformity\* --  
Chi-squared Statistic

Cell	Expected Count	Run 1	Run 2	Run 3	Run 4	Run 5
1	10	2.5	3.6	0.1	0.4	0.1
2	10	0.9	0.9	0.9	0.1	3.6
3	10	0.4	0.1	0.0	0.1	0.1
4	10	0.4	0.4	0.1	0.1	0.4
5	10	0.4	0.0	0.9	0.1	3.6
6	10	0.4	0.1	0.4	3.6	0.0
7	10	2.5	0.1	0.1	0.1	0.1
8	10	0.9	2.5	3.6	0.9	0.4
9	10	1.6	0.4	0.4	0.9	0.1
10	10	0.0	0.1	0.1	0.1	0.4
Totals:		10.0	8.2	6.6	6.4	8.8

\*Notes:

Level of Significance = 0.05  
Critical Value for Chi-squared: 16.9

### The Simulation

Unfortunately, having found the underlying distributions for C and N was not enough to set up a valid simulation for specimen lives. Individual values were easily generated to match the distributions desired, but the random pairing of C and N values (which assumes independence) led to huge errors in predicting the lives of the same specimens which provided the original data. An analysis of the covariance between  $\ln(C)$  and N showed a strong relationship between the two values. (One should expect the slope and intercept of a straight line to be related!)

The covariance was determined as follows:

$$\sigma_{12} = E(x*y) - E(x) * E(y) \quad (A13)$$

$$\rho_{12} = \sigma_{12} / \sigma_1 \sigma_2 \quad (A14)$$

where

$$x = \ln(C)$$

$$y = N$$

therefore,

$$E(x) = -18.6938$$

$$\sigma_1 = 0.6848$$

$$E(y) = 2.6204$$

$$\sigma_2 = 0.2745$$

$$E(x*y) = -49.1724$$

$$\sigma_{12} = -0.1872$$

and finally,

$$\begin{aligned} \rho_{12} &= (-0.1872) / [(0.6848)(0.2745)] \\ &= -0.9957 \end{aligned}$$

Since values obtained for C and N are not independent, they cannot be randomly paired during the simulation. However, the extremely high (-0.996) magnitude of covariance for ln(C) vs N indicates a very strong linear relationship. Therefore, a least squares linear regression was accomplished for ln(C) as a function of N.

The fit resulted in a correlation coefficient (r) of 0.996 which corresponds, as it should, with the covariance between the two variables. The coefficient of determination ( $r^2$ ) was 0.991. Using these values, the appropriate value for C was expressed as a function of N as follows:

$$C = \exp[(-2.484)N - 12.86] \quad (A15)$$

However, even though the fit for ln(C) vs N was very good, the relationship is not perfectly linear. The error term from the regression had to be considered.

Since the sum of error terms about a regression line must be zero, the mean error must be zero. Also, since the sample size is large, the error terms can be assumed to be normally distributed. Finally, the mean square error (sample variance) must be determined. Reference 9 provided a useful equation for MSE, also known as  $s^2$ .

$$s^2 = \frac{\sum y_i^2 - b_0 \sum y_i - b_1 \sum x_i y_i}{n-2} \quad (A16)$$

where

n = total number of data points

Solving Equation A16 provided the random variable necessary to generate C as a function of N.

$$C = \exp[(-2.484)N - 12.86 + \epsilon] \quad (A17)$$

where  $\epsilon$  is normally distributed with a mean of zero and a standard deviation of 0.66.

Having defined the random variables C and N, and a mean and standard deviation for  $\epsilon$ , the simulation software was developed.

Simulation Software. The simulation of specimen lives was run on an 8-bit PCC 2000 microcomputer (with an 8085 microprocessor). The program was written in MBASIC and is relatively easy to understand. Two sections are explained below.

Box-Muller Technique. The subroutine to generate standard normal variates (lines 900 - 980) used the Box-Muller transform. A complete description of this technique is given on pages 315-316 of Reference 2.

Growth Rate Calculations. The objective of this simulation was to generate specimen lives (number of elapsed load cycles) under simulated constant amplitude cyclic fatigue. Initial and final half crack lengths of 0.5 and 1.5 inches, respectively, were chosen to indicate the start and end of a specimen's "life" for this study. Before these values are meaningful, though, they must be expressed in terms of the independent variable of interest --  $\Delta K$ .

$$\Delta K = \Delta \sigma (\pi a)^{1/2} [1 + 0.256(a/w) - 1.152(a/w)^2 + 12.19(a/w)^3] \quad (A18)$$

where

a = Half crack length (inches)  
w = Specimen width (inches)  
 $\Delta \sigma$  = Delta stress (max-min, ksi)

For this study,

$\Delta \sigma = 7.0$  ksi  
w = 6.0 inches

Therefore, the initial value of  $\Delta K$  for a crack length of 0.5 inches was 8.87. The final  $\Delta K$  value at a crack length of 1.5 inches was 17.55. Using these values in the Walker equation along with the fixed values of  $R=0.2$  and  $m=0.682$ :

$$\begin{aligned} \left( \frac{da}{dn} \right)_i &= C [(8.87)(0.8)^{(-0.318)}]^N \\ &= C(9.52)^N \end{aligned} \quad (A19)$$

$$\begin{aligned} \left( \frac{da}{dn} \right)_f &= C [(17.55)(0.8)^{(-0.318)}]^N \\ &= C(18.84)^N \end{aligned} \quad (A20)$$

which are the initial and final crack growth rates.

Since the growth rate curve is linear for the above range of  $\Delta K$  values, the "effective" growth rate is simply the average of the end points.

$$\log \left( \frac{da}{dn} \right)_{\text{eff}} = \frac{\log \left( \frac{da}{dn} \right)_i + \log \left( \frac{da}{dn} \right)_f}{2} \quad (\text{A21})$$

The overall growth rate can then be approximated by dividing the change in crack length by the change in cycle count.

$$\frac{\Delta a_i}{\Delta n_i} = \left( \frac{da}{dn} \right)_{\text{eff}} \quad (\text{A22})$$

or

$$\Delta n_i = \frac{\Delta a_i}{\left( \frac{da}{dn} \right)_{\text{eff}}} \quad (\text{A23})$$

Knowing that  $\Delta a = (1.5 - 0.5) = 1.0$ , the life of a given specimen is

$$\Delta N = \left( \frac{da}{dN} \right)_{\text{eff}}^{-1} \quad (\text{A24})$$

The Program Listing. The next three pages contain a complete listing of the MBASIC program (Figure A6). The program produced two samples of 68 data points for each of 10 trials.

```

10 '*****
20 '**** MATERIAL PROPERTIES SIMULATION ****
30 '**** RODNEY L. WILKINSON ****
40 '*****
50 CLEAR
60 SIZE=68: 'SAMPLE SIZE
70 DIM R(SIZE+1),Z(SIZE+1),N(2,SIZE),E(SIZE),C(2,SIZE)
71 DIM L(2,SIZE)
80 DIM NSUM(2),CSUM(2),LSUM(2),N2SUM(2),C2SUM(2),L2SUM(2)
81 DIM NVAR(2),CVAR(2),LVAR(2)
90 '
100 PI = 3.14159 : X = LOG(10)
110 NMEAN = 2.6204 : NDEV = .274513
120 EDEV = .065956 : 'EMEAN = 0
130 B0 = -12.1859 : B1 = -2.48355
140 ALPHA = 2.7369 : BETA = 11.8386
150 '
160 INPUT"HOW MANY TRIALS ";TRIALS
170 FOR K=1 TO TRIALS
180 '
190 GOSUB 820: 'FILL RANDOM NUMBER ARRAY ***
200 GOSUB 900: 'GENERATE RANDOM VARIATES ***
210 '
220 '***** CALCULATE VALUES FOR N *****
230 '
240 '- NORMAL -
250 FOR I=1 TO SIZE
260 N(1,I)=NMEAN+NDEV*Z(I)
270 NEXT I
280 '
290 '- WEIBULL -
300 FOR I=1 TO SIZE
310 N(2,I)=ALPHA*(-LOG(1-R(I)))^(1/BETA)
320 NEXT I
330 '
340 GOSUB 820: 'FILL RANDOM NUMBER ARRAY ***
350 GOSUB 900: 'GENERATE RANDOM VARIATES ***
360 '
370 '***** CALCULATE VALUES FOR E *****
380 FOR I=1 TO SIZE
390 E(I)= 0 + EDEV*Z(I)
400 NEXT I
410 '
420 '***** CALCULATE VALUES FOR C *****
430 FOR I=1 TO SIZE
440 C(1,I)=EXP(B0+B1*N(1,I)+E(I))
450 C(2,I)=EXP(B0+B1*N(2,I)+E(I))
460 NEXT I

```

Figure A6. Simulation Program Listing

```

470 '
480 '***** CALCULATE GROWTH RATES *****
490 FOR J=1 TO 2
500 FOR I=1 TO SIZE
510 Y1=C(J,I)*( 9.52)^N(J,I) : ' INITIAL GROWTH RATE
520 Y2=C(J,I)*(18.84)^N(J,I) : ' FINAL GROWTH RATE
530 Y=10^(((LOG(Y1)/X)+(LOG(Y2)/X))/2) : 'AVERAGE RATE
540 L(J,I)=1/Y : ' LIFE FROM 0.5" TO 1.5" (CYCLES)
550 NEXT I:NEXT J
560 '
570 '***** CALCULATE MEANS & STD DEVS *****
580 FOR J=1 TO 2
590 FOR I=1 TO SIZE
600 NSUM(J)=NSUM(J)+N(J,I)
601 CSUM(J)=CSUM(J)+C(J,I)
602 LSUM(J)=LSUM(J)+L(J,I)
610 N2SUM(J)=N2SUM(J)+N(J,I)^2
611 C2SUM(J)=C2SUM(J)+C(J,I)^2
612 L2SUM(J)=L2SUM(J)+L(J,I)^2
620 NEXT I
630 NSUM(J)=NSUM(J)/SIZE
631 CSUM(J)=CSUM(J)/SIZE
632 LSUM(J)=LSUM(J)/SIZE
640 N2SUM(J)=N2SUM(J)/SIZE
641 C2SUM(J)=C2SUM(J)/SIZE
642 L2SUM(J)=L2SUM(J)/SIZE
650 NVAR(J)=N2SUM(J)-NSUM(J)^2
651 CVAR(J)=C2SUM(J)-CSUM(J)^2
652 LVAR(J)=L2SUM(J)-LSUM(J)^2
660 NEXT J
670 '
680 '***** PRINT OUTPUT *****
690 LPRINT"TRIAL ";K," NORMAL FIT"," WEIBULL FIT"
700 LPRINT," MEAN"," STD DEV"," MEAN"," STD DEV"
710 LPRINT" SLOPE (N)",NSUM(1),SQR(NVAR(1)),NSUM(2),
711 LPRINT SQR(NVAR(2))
720 LPRINT"INTERCEPT (C)",CSUM(1),SQR(CVAR(1)),CSUM(2),
721 LPRINT SQR(CVAR(2))
730 LPRINT" LIFE ",LSUM(1),SQR(LVAR(1)),LSUM(2),
731 LPRINT SQR(LVAR(2))
740 LPRINT
750 GOSUB 1000
760 ERASE NSUM,CSUM,LSUM,N2SUM,C2SUM,L2SUM,NVAR,CVAR,LVAR
770 NEXT K
780 END
790 '

```

Figure A6 (Continued)

---

```

800 '***** SUBROUTINES *****
810 '
820 '***** GENERATE RANDOM NUMBERS
830 FOR I=1 TO SIZE+1
840 R(I)=RND(1)
850 NEXT I
860 RETURN
870 '
900 '***** BOX-MULLER TRANSFORM TO CREATE NORMAL VARIATES
910 HALF=INT(SIZE/2+.5)
920 FOR I=1 TO HALF
930 A= (-2*LOG(R(I)))^.5
940 B= (2*PI*R(I+HALF))
950 Z(I) = A*COS(B)
960 Z(I+HALF)=A*SIN(B)
970 NEXT I
980 RETURN
990 '
1000 '***** SAVE DATA ON DISK *****
1010 OPEN"O",1,"TRIAL"+MID$(STR$(K),2)
1020 PRINT#1,SIZE
1030 FOR I=1 TO SIZE
1040 PRINT#1,L(1,I),L(2,I)
1050 NEXT I
1060 CLOSE
1070 RETURN

```

---

Figure A6 (Concluded)

## Output Analysis

The first step in evaluating the simulation output was to compare sample means and variances with those from measured data.

Test for Equality of Variances. Since a statistical comparison of means requires knowledge of whether variances are equal, the variances were evaluated first. The distribution of measured lives will be discussed later, but for now, it is important to note that it does not appear to be normal.

Without the assumption of population normality, a large sample procedure was required to evaluate the equality of sample variances. Regardless of underlying population distributions, the standard deviations of large samples follow approximately normal distributions (9:313).

$$Z = \frac{s_1 - s_2}{s_p \sqrt{\frac{1}{2n_1} - \frac{1}{2n_2}}} \quad (A25)$$

where

$$n_1 = n_2 = 68$$
$$s_p = \sqrt{\frac{(n_1-1)s_1^2 + (n_2-1)s_2^2}{n_1 + n_2 - 2}} \quad (A26)$$

Variances from each trial were compared to the variance of measured data. As is shown in Table A9, the variances of all trials were considered equal to the

variance of the measured data at a 0.05 level of significance. The critical Z-value was  $\pm 1.96$ .

Test for Equality of Means. Based on the above Z test, the assumption of equal variances is valid. Consequently, the pooled estimator ( $S_p$ ) from Equation A26 was used to represent the overall population standard deviation. Also, trial means were assumed to be normally distributed based on the Central Limit Theorem. The pooled T test was then used to evaluate the equality of sample means,

$$T = \frac{\bar{x} - \bar{y} - \Delta}{S_p \sqrt{\frac{1}{n_1} + \frac{1}{n_2}}} \quad (A27)$$

The entire simulation was based on 68 least squares curve fits. However, average specimen life calculated using the regression formulas was about five percent less than the average measured life. Given the inherent variability in fatigue crack growth, such an error is quite acceptable -- especially since the error leads to conservative results (predicts shorter lives). The slack variable,  $\Delta$ , was introduced to account for regression error. By eliminating the regression error, the validity of simulation results could be meaningfully evaluated.

$$\Delta = (.05)(154063) = 7703 \text{ cycles}$$

The pooled T test was conducted at the 0.05 level of significance with  $\nu = 134$  degrees of freedom. The critical T value for these parameters was  $\pm 1.96$ . These results are also shown in Tables A9 and A10.

Table A9: Test for Equality of Means and Variances\* --  
Normal Variates

Trial	Mean	Std Dev	Z-value	T-value
1	146432	11365	-0.02	-0.04
2	149001	11920	-0.41	-1.32
3	145259	9537	1.42	0.61
4	145376	11016	0.24	0.51
5	143933	10868	0.35	1.27
6	147719	10551	0.60	-0.72
7	145932	10370	0.74	0.23
8	146534	9352	1.58	-0.10
9	146940	11564	-0.16	-0.30
10	147069	9511	1.44	-0.40

Table A10: Test for Equality of Means and Variances\* --  
Weibull Variates

Trial	Mean	Std Dev	Z-value	T-value
1	147203	12869	-1.04	-0.41
2	148886	11234	-0.78	-1.30
3	146098	9425	1.52	0.15
4	145887	10077	0.97	0.26
5	144211	9797	1.20	1.18
6	148260	12037	-0.49	-0.95
7	147870	10083	0.97	-0.82
8	146342	9742	1.25	0.01
9	147302	10945	0.29	-0.49
10	148174	9643	1.33	-1.00

\* Notes:

Evaluated against a mean of 154,063 (T-Test)  
standard deviation of 11,340.2 (Z-Test)  
at a level of significance of 0.05.  
The critical values for Z and T were  $\pm 1.96$ .

As is shown in Tables A9 and A10, all trial means and variances passed equality testing. Therefore, the simulated lives were within five percent of the measured values. Variances for all trials were essentially equal to the measured variance. Also, based on Tables A9 and A10, there appeared to be no significant difference between predictions made with the normal and Weibull random variates. Since the normal distribution is more convenient to work with, material properties for the main thesis simulation were based on the normal variates.

Comparing Distributions. As mentioned earlier, the distribution of measured lives was not normal. The distribution appeared to be lognormal, but only weakly so. Table A11 shows the goodness of fit test for the lognormal distribution.

Table A11: Chi-squared fit for Normal Distribution<sup>\*</sup>  
of  $\ln(\text{Life})$

Cell	Upper Bound	Expected Number	Observed Number	Chi-squared Statistic
1	11.883	13.6	14	0.012
2	11.925	13.6	17	0.850
3	11.961	13.6	11	0.497
4	12.002	13.6	14	0.012
5	Infinity	13.6	12	0.188
		68.0	68	1.559

<sup>\*</sup> Notes:

Mean = 11.943                      Std Dev = 0.071

Level of Significance = 0.05

Critical Value for Chi-Squared = 5.99

Unfortunately, attempts to confirm a relationship between the underlying distributions for measured and simulated lives failed. Figures A7 through A10 show the histogram of measured lives, along with the histograms for lives calculated by the regression, and the two simulated outputs from Trial 1. Note that in both cases, the simulated data appears to have a definite leftward skew as compared to the measured data. This is the type of error desired in life prediction techniques because it yields conservative results -- predicting shorter structural lives rather than longer ones.

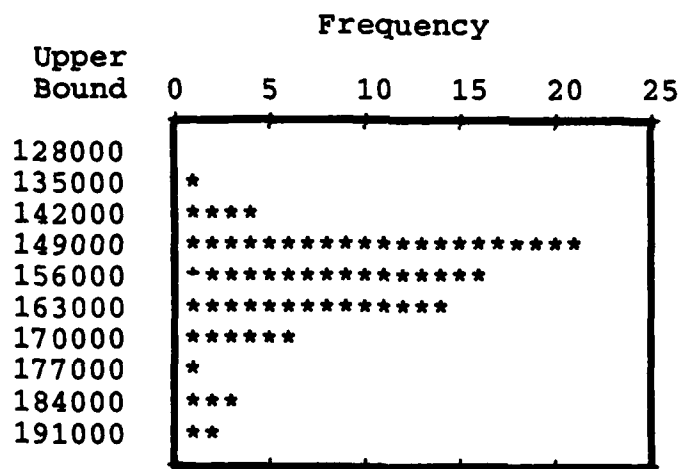


Figure A7. Histogram for Measured Lives

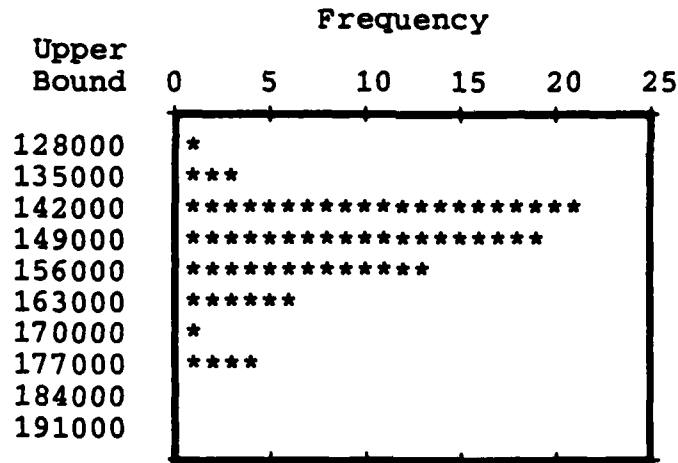


Figure A8. Histogram for Lives Obtained by Regression

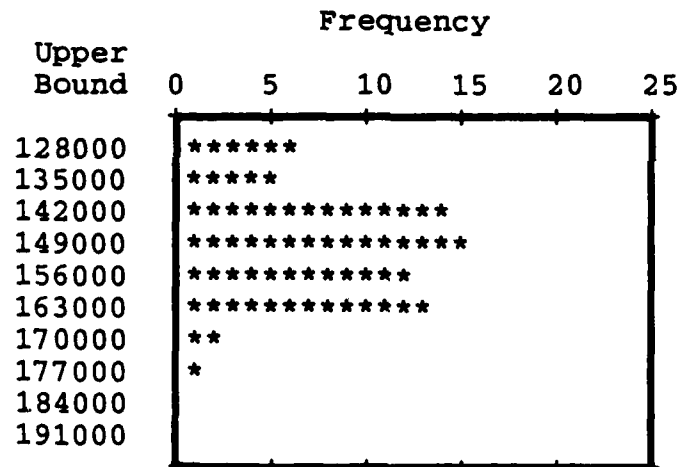


Figure A9. Histogram for Lives Simulated Based on a Normal Distribution for N

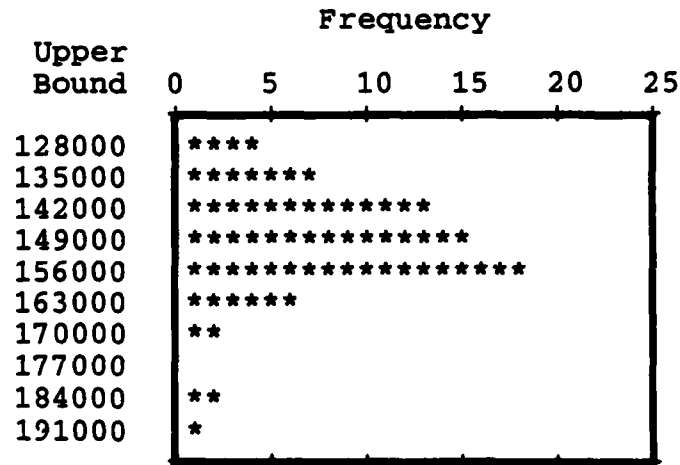


Figure A10. Histogram for Lives Simulated Based on a Weibull Distribution for N

## Conclusions

The material properties simulation provided an excellent estimate of specimen crack growth lives. Sample overall means for measured and simulated data were within five percent of each other, and almost all of the error was due to the regression fit. Variances for all data groups were essentially equal. The small error that did result from the regression and simulation procedures yielded conservative predictions. Therefore, the process described in this appendix was used to generate material properties data for the thesis simulation.

## Appendix B: CRACKS4: A Life Prediction Model

The model used to conduct structural life simulations was CRACKS4, an Air Force computer code developed by Mr. R.M. Engle, Jr. The CRACKS4 code is extensive and is only superficially described here. Please refer to References 11 and 14 for detailed information.

CRACKS4 is the latest version of the original CRACKS program released in 1970. The model has been thoroughly validated during 15 years of use by the Air Force. A brief synopsis of versions II through IV is provided below.

The CRACKS II computer program is a specialized integration routine, which determines incremental crack growth for each of a series of discrete load levels, given a stress intensity factor formulation and crack growth rate relationship. CRACKS II provides the additional capability of modeling load interaction effects (crack growth retardation). At the present time, three models are available; the Wheeler model, the Willenborg model, and a . . . closure model. Further flexibility is provided through three crack growth rate relationships . . . At present the program also provides nine stress intensity factor formulations ranging from a center cracked finite width sheet to a corner flaw from a fastener hole.

For each load level in the spectrum, CRACKS II determines the stress intensity  $K_{max}$ , or the stress intensity range  $\Delta K$ , corresponding to the current crack length. These values then are modified by the load interaction model to account for retardation effects. The resulting "effective"  $K_{max}$  or  $\Delta K$  then is used in conjunction with one of the preceding growth rate relationships to determine the incremental crack growth. The crack growth increments are then summed to give crack growth vs cycles. (13)

Figure B1 schematically shows the input parameters and relationships used for a CRACKS4 program run. By combining available input parameters and crack growth relationships, very complicated structural configurations and load histories can be effectively modeled.

The output for the baseline thesis run of CRACKS4 is presented in Figure B2. Similar runs were accomplished for each of the 180 conditions simulated during the thesis. Note that the analysis is based on individual load cycles. A block represents one application of the input load history, which in this case was 30,795 cycles (150 flight hours).

Anyone desiring more information on the CRACKS4 program or the outputs generated for this thesis should contact Mr. R.M. Engle at the address listed in Figure B2.

# **CURRENT ANALYSIS CAPABILITY VARIABLE AMPLITUDE GROWTH PREDICTION** FRACTURE MECHANICS APPROACH

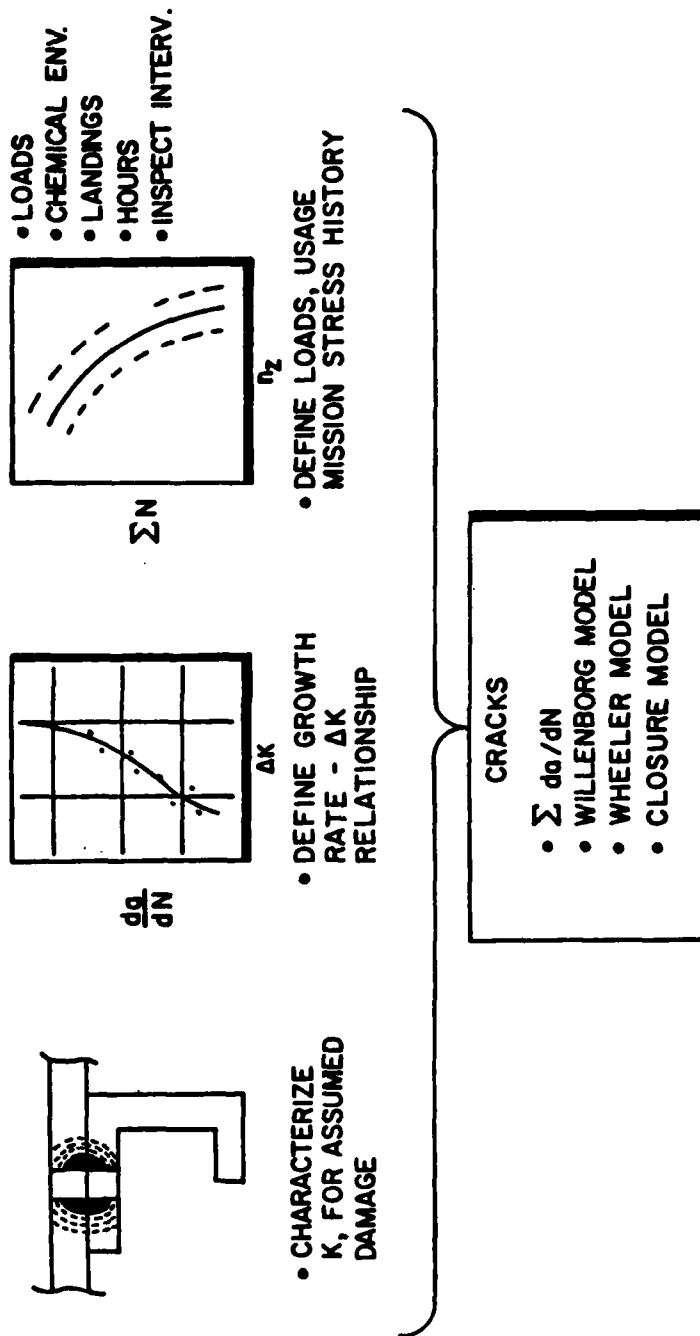


Figure B1. Schematic of CRACKS4 Inputs

\*\*\*\*\* CRACKS IV \*\*\*\*\*

AFFDL(FBE)  
ATTN(R.M.ENGLE JR.)  
W-PAFB,OHIO 45433

#####

#####

\*\*\*\*\*

**CASE 1 RUN 1**

\*\*\*\*\*

**THESIS SIMULATION (BASELINE RUN, 150 FLT HRS/BLOCK)**

## CRACK PROPAGATION ANALYSIS USING WALKER'S EQUATION

$$DA/DN=C*(DELTA\ K/((1-R)**(1-M)))*N$$

WHERE K IS OF THE FORM ....  $K = \text{SIGMA} * \text{SORT}(\text{PI} * A) * \text{BETA}$

### AVERAGE MATERIAL PROPERTIES FROM VIRKLER DATA

C = 0.74030000E-08      M = 0.6820      N = 2.631

KSUBQ = 0.65000000E+02      YIELD STRESS = 0.50000000E+02

INITIAL HALF CRACK LENGTH = 0.12500000E+00

INITIAL CYCLE NUMBER = 0.00

R CUTOFF = 0.800

**AUTOMATIC UNRETARDED SOLUTION SUPPRESSED**

## EFFECTIVE STRESS RETARDATION MODEL

### RETARDATION MODEL MODIFIED BY RELAXATION FUNCTION

$$PHI = (1-THRESHOLD/K \text{ MAX})/(2.30-1)$$

PLANE STRESS YIELD ZONE CONDITION ASSUMED

CORRECTION FACTOR BETA(1) IS A CONSTANT

```
BETA(1) = 0.400000000E-01
```

APPLIED FROM A= 0.12500000E+00 TO A = 0.10000000E+06

CORRECTION FACTOR BETA(2) IS FINITE WIDTH CORRECTION

```
BETA(2) = SORT(SEC(PI*A/B))
```

WHERE THE EFFECTIVE PLATE WIDTH W = 0.40000000E+01

APPLIED FROM A = 0.12500000E+00 TO A = 0.10000000E+06

CORRECTION FACTOR BETA(6) IS UNIAXIAL BOWIE SOLUTION FOR TWO CRACKS

FROM A CIRCULAR HOLE OF RADIUS R = 0.12500000E+00

APPLIED FROM A = 0.12500000E+00 TO A = 0.10000000E+06

**BASELINE STRESS HISTORY (150 FLT HRS/BLOCK)**

## 10000 BLOCKS IN SPECTRUM

\*\*\*\*\*END OF INPUT\*\*\*\*\*

**Figure B2. Sample Output from CRACKS4 Program**



END OF BLOCK 9		CRACK LENGTH =	0.20428
GROWTH THIS BLOCK =	0.00995	TOTAL GROWTH =	0.07928
END OF BLOCK 10		CRACK LENGTH =	0.21463
GROWTH THIS BLOCK =	0.01035	TOTAL GROWTH =	0.08963
END OF BLOCK 11		CRACK LENGTH =	0.22540
GROWTH THIS BLOCK =	0.01076	TOTAL GROWTH =	0.10040
END OF BLOCK 12		CRACK LENGTH =	0.23660
GROWTH THIS BLOCK =	0.01121	TOTAL GROWTH =	0.11160
END OF BLOCK 13		CRACK LENGTH =	0.24827
GROWTH THIS BLOCK =	0.01167	TOTAL GROWTH =	0.12327
END OF BLOCK 14		CRACK LENGTH =	0.26044
GROWTH THIS BLOCK =	0.01217	TOTAL GROWTH =	0.13544
END OF BLOCK 15		CRACK LENGTH =	0.27314
GROWTH THIS BLOCK =	0.01270	TOTAL GROWTH =	0.14814
END OF BLOCK 16		CRACK LENGTH =	0.28640
GROWTH THIS BLOCK =	0.01326	TOTAL GROWTH =	0.16140
END OF BLOCK 17		CRACK LENGTH =	0.30026
GROWTH THIS BLOCK =	0.01386	TOTAL GROWTH =	0.17526
END OF BLOCK 18		CRACK LENGTH =	0.31477
GROWTH THIS BLOCK =	0.01451	TOTAL GROWTH =	0.18977
END OF BLOCK 19		CRACK LENGTH =	0.32997
GROWTH THIS BLOCK =	0.01520	TOTAL GROWTH =	0.20497
END OF BLOCK 20		CRACK LENGTH =	0.34591
GROWTH THIS BLOCK =	0.01594	TOTAL GROWTH =	0.22091
END OF BLOCK 21		CRACK LENGTH =	0.36266
GROWTH THIS BLOCK =	0.01675	TOTAL GROWTH =	0.23766

---

Figure B2. (Continued)

END OF BLOCK 22		CRACK LENGTH =	0.38028
GROWTH THIS BLOCK =	0.01762	TOTAL GROWTH =	0.25528
END OF BLOCK 23		CRACK LENGTH =	0.39885
GROWTH THIS BLOCK =	0.01857	TOTAL GROWTH =	0.27385
END OF BLOCK 24		CRACK LENGTH =	0.41846
GROWTH THIS BLOCK =	0.01961	TOTAL GROWTH =	0.29346
END OF BLOCK 25		CRACK LENGTH =	0.43920
GROWTH THIS BLOCK =	0.02074	TOTAL GROWTH =	0.31420
END OF BLOCK 26		CRACK LENGTH =	0.46120
GROWTH THIS BLOCK =	0.02200	TOTAL GROWTH =	0.33620
END OF BLOCK 27		CRACK LENGTH =	0.48459
GROWTH THIS BLOCK =	0.02339	TOTAL GROWTH =	0.35959
END OF BLOCK 28		CRACK LENGTH =	0.50952
GROWTH THIS BLOCK =	0.02494	TOTAL GROWTH =	0.38452
END OF BLOCK 29		CRACK LENGTH =	0.53620
GROWTH THIS BLOCK =	0.02668	TOTAL GROWTH =	0.41120
END OF BLOCK 30		CRACK LENGTH =	0.56485
GROWTH THIS BLOCK =	0.02865	TOTAL GROWTH =	0.43985
END OF BLOCK 31		CRACK LENGTH =	0.59576
GROWTH THIS BLOCK =	0.03091	TOTAL GROWTH =	0.47076

\*\*\*\*\*  
KMAX APPLIED EXCEEDS KSUBQ. PROBLEM TERMINATED  
\*\*\*\*\*

---

Figure B2. (Continued)

LAST CALCULATED VALUES ARE

BLOCK IN SPECTRUM	32
SEGMENT NUMBER	1
MISSION NUMBER	1
FLIGHT NUMBER	96457
LAYER IN MISSION	9768
ACCUMULATED CYCLES	0.96425700E+06
CRACK LENGTH	0.60973419E+00
KMAX APPLIED	0.65060888E+02
KMAX EFFECTIVE	0.65060888E+02
DELTA K	0.34612392E+02
DA/DN	0.00000000E+01

\*\*\*\*\*CPU TIME= 58MINS 23.31SECS \*\*\*\*\*

---

Figure B2. (Concluded)

## Appendix C: A Formula for Structural Life?

In Chapter V, a strong quantifiable relationship was demonstrated between the Walker slope, stress level, and structural life. That relationship will not be applicable to other simulations until it is generalized by including the stress intensity factor,  $\Delta K$ . Development of the complete relationship is beyond the scope of this thesis. This appendix explains the conditions under which the relationship was derived, and provides a basis for future work on a generalized formula.

Equation 7 (page 78) predicted structural life for a single structural geometry based on five very similar load histories. Therefore, the equation is only good for a very limited range of initial and final stress intensity factors. To account for varying geometries and load histories, the stress intensity factor must be incorporated directly into the regression used to derive Equation 7. Since the stress intensity factor is a function of structural loads and geometry, those parameters must be fully defined before the equation can be generalized.

The load histories were described using root-mean-square (RMS) stresses. The relative severity of load histories can often be evaluated by comparing RMS values. RMS stresses were calculated as follows:

$$\sigma_{\text{RMS}} = \left[ \frac{\sum (\sigma_i)^2}{n} \right]^{1/2} \quad (\text{C1})$$

where

$\sigma_{\text{RMS}}$  = Root-mean-square stress (ksi)

$\sigma_i$  = Stress level for an individual cycle (ksi)

$n$  = Number of cycles in load history

Note that the above equation applies to valley, peak, or delta stresses depending on the values used for  $\sigma_i$ . The values for stress were further generalized to avoid calculating RMS values for each design limit stress. Table C1 shows RMS factors for each of the five load histories used in this study. To determine a particular RMS stress from the table, multiply the design limit stress by the RMS factor to obtain the desired stress. For example, the baseline load history at a design limit stress of 40 ksi would have an RMS peak stress of  $(40)(.2744) = 10.976$  ksi.

Table C1: Root-mean-square Factors for Load Histories

Load History	Peak RMS Factor	Valley RMS Factor	Delta RMS Factor
Baseline	0.2744	0.1117	0.1783
RF2	0.2703	0.1061	0.1889
RMP1F	0.2741	0.1111	0.1776
RMP1	0.2742	0.1112	0.1770
RMP2	0.2555	0.1040	0.1680

Once the relative severity of load histories was defined, the effects of geometry on the stress intensity factor were evaluated. In general, the stress intensity factor is defined as

$$K = \sigma \sqrt{\pi a} \beta \quad (C2)$$

where  $\beta$  represents the product of various geometrical correction factors. Two correction factors were used during the simulation. The first,  $\beta_1$ , was a finite width correction to account for the crack growth behavior near the edge of a plate. The second,  $\beta_2$ , was Grandt's approximation to the Bowie solution for a remotely loaded hole with diametric cracks. For more information on the correction factors, please refer to Reference 15. Formulas for  $\beta_1$  and  $\beta_2$  are listed below.

$$\beta_1 = 1 + 0.256(a/w) - 1.152(a/w)^2 + 12.19(a/w)^3 \quad (C3)$$

$$\beta_2 = \frac{0.6866}{0.2772 + (a/r)} + 0.9439 \quad (C4)$$

where

a = Crack length from edge of hole (one side)  
w = Plate width (inches)  
r = Hole radius (inches)

Knowing that the hole radius was 0.125 inches and the plate width was 4.0 inches, the above equations were used to

calculate the initial RMS stress intensity factor ( $\Delta K_i$ ) for the assumed crack length of 0.125 inches. Finding the final RMS value,  $\Delta K_f$ , was not so easy.

Based on the material fracture toughness of  $65 \text{ ksi}\sqrt{\text{in}}$ , the critical crack length was calculated by substituting the appropriate value for design limit stress into Equation C2 and iterating to find  $a_{\text{crit}}$ . The calculated  $a_{\text{crit}}$  was then used along with  $\Delta\sigma_{\text{RMS}}$  to determine the final stress intensity. Resulting values for the baseline load history are presented in Table C2. (Values for  $\Delta\sigma_{\text{RMS}}$  were obtained using Table C1.)

Table C2: Selected Parameters for Baseline Load History

Parameter	Design Limit Stress		
	38 ksi	40 ksi	42 ksi
$\Delta\sigma_{\text{RMS}}$	6.774	7.131	7.487
$a_{\text{crit}}$	0.714	0.649	0.589
$\Delta K_i$	6.335	6.668	7.001
$\Delta K_f$	11.581	11.578	11.584

The information in Table C2 can be reproduced for several combinations of stress level, crack length, and geometry. Once an adequate amount of data is available, the multiple regression used to generate Equation 7 could be expanded, and has the potential to provide a generalized formula for structural life.

In summary, a formula for structural life should be determined by multiple regression with the following independent variables: (1) The Walker slope  $N$ , (2) the RMS spectrum stress, (3) the initial stress intensity factor, and (4) the final stress intensity factor. Stress intensity factors should be calculated based on the RMS stress using initial and final crack lengths. The final crack length does not necessarily have to be  $a_{crit}$ .

If the regression is successful in producing a general formula for life, the resources required to repeat this thesis simulation could be reduced from 180 CPU hours to less than one CPU minute. Further work in this area is certainly warranted.

## Bibliography

1. Allen, Phil. Ogden Air Logistics Center (OO-ALC/MMSRA), Hill AFB UT. Interview. April 1985.
2. Banks, J. and J.S. Carson, II. Discrete Event System Simulation. Englewood Cliffs NJ: Prentice-Hall, 1984.
3. Benjamin, J.R. and C.A. Cornell. Probability, Statistics, and Decision for Civil Engineers. New York: McGraw-Hill, 1970.
4. Berens, A.P. and others. Handbook of Force Management Methods. AFWAL-TR-81-3079. Wright-Patterson AFB OH: Air Force Wright Aeronautical Laboratories, April 1981.
5. Carter, J.P. "STEMS Structural Tracking and Engine Monitoring System," Worldwide Air Force Structural Integrity Conference Final Report, 35-37 (1983).
6. Christian, Thomas F., Jr. Warner Robins Air Logistics Center (WR-ALC/MMSRD), Robins AFB GA. Multiple Interviews, August 1984 - April 1985.
7. Clay, L.E. and others. Force Management Methods Task 1 Report--Current Methods. AFFDL-TR-78-183. Wright-Patterson AFB OH: Air Force Flight Dynamics Laboratory, December 1978.
8. Department of the Air Force. Aircraft Structural Integrity Program. AFR 80-13. Washington: HQ USAF, July 1976 and October 1984.
9. DeVore, J.L. Probability and Statistics for Engineering and the Sciences. Monterey CA: Brooks/Cole, 1982.
10. Ebeling, C. Air Force Institute of Technology (AFIT/ENS), Wright-Patterson AFB OH. Privately developed software. March 1985.
11. Engle, Robert M., Jr. AFWAL/FIBEC, Wright-Patterson AFB OH. Multiple Interviews, June 1984 - July 1985.
12. Engle, R.M., Jr. and T.F. Christian, Jr. Maintenance Impact of Current Loads Recording Methodology on Crack-Growth Based Individual Aircraft Tracking. San Diego CA: Proceedings of AIAA/AHS/ASEE Aircraft Design Systems and Operations Meeting. American Institute of Aeronautics and Astronautics, 1984

13. Engle, R.M., Jr. and J.L. Rudd. "Spectrum Crack Growth Analysis Using the Willenborg Model," Journal of Aircraft 13 (7): 462-466 (July 1976).
14. Engle, R.M., Jr. CRACKS, A Fortran IV Digital Computer Program for Crack Propagation Analysis. AFFDL-TR-70-107. Wright-Patterson AFB OH: Air Force Flight Dynamics Laboratory, 1970.
15. Gallagher, J.P. USAF Damage Tolerant Design Handbook: Guidelines for the Analysis and Design of Damage Tolerant Aircraft Structures. AFWAL-TR-82-3073. Wright-Patterson AFB OH: Air Force Wright Aeronautical Laboratories, May 1984.
16. Giessler, F.J. and J.P. Gallagher. Evaluation of the Crack Growth Gage Concept as an Individual Aircraft Tracking Device. AFWAL-TR-83-3082, Vol 1. Wright-Patterson AFB OH: Air Force Wright Aeronautical Laboratories, September 1983.
17. Guadagnino, C.L. Evaluation of a Damage Accumulation Monitoring System as an Individual Aircraft Tracking Concept. AFWAL-TR-82-3023. Wright-Patterson AFB OH: Air Force Wright Aeronautical Laboratories, May 1982.
18. Howard, Harold W., Ed Davidson, and David Erskine. Aeronautical Systems Division (ASD/ENFSF), Wright-Patterson AFB OH. Interview, April 1985.
19. Hudson, C.M. Effects of Stress Ratio on Fatigue Crack Growth in 7075-T6 and 2024-T3 Aluminum. NASA-TN-D5390. 1969.
20. Lincoln, John W. ASD/ENFS, Wright-Patterson AFB OH. Interview, August 1984.
21. Markland, R.E. Topics in Management Science (Second Edition). New York: John Wiley and Sons, 1983.
22. Negaard, G. R. The History of the Aircraft Structural Integrity Program. ASIAC Report No. 680.1B. Wright-Patterson AFB OH: Aerospace Structures Information and Analysis Center, June 1980.
23. Ostergaard, D.F. Characterization of the Variability in Fatigue Crack Propagation Data. MS Thesis, Purdue University, W. Lafayette IN, 1981.
24. Paris, P.C. "The Fracture Mechanics Approach to Fatigue," Fatigue -- an Interdisciplinary Approach, 107-132. Syracuse NY: Syracuse University Press, (1964).

25. Parker, G.S. Generalized Procedures for Tracking Crack Growth in Fighter Aircraft. AFFDL-TR-76-133. Wright-Patterson AFB OH: Air Force Flight Dynamics Laboratory, January 1977.
26. Rudd, J.L. "Air Force Damage Tolerance Design Philosophy", Damage Tolerance of Metallic Structures: Analysis, Methods, and Applications. Philadelphia: American Society for Testing and Materials, ASTM STP 842: p 134-141 (1984).
27. Rudd, J. L. and others. "Part-Through Crack Problems in Aircraft Structures," Part-Through Crack Problems in Aircraft Structures. Philadelphia: American Society for Testing and Materials, ASTM STP 687: 168-194 (1979).
28. Special Working Papers (Available from Reference 11.)
29. Virkler, D.A. and others. The Statistical Nature of Fatigue Crack Propagation. AFFDL-TR-78-43 (Data Volume). Wright-Patterson AFB OH: Air Force Flight Dynamics Laboratory, April 1978.
30. Walker, E.K. "The Effects of Stress Ratio During Crack Propagation and Fatigue for 2024-T3 and 7075-T6 Aluminum," Effects of Environment and Complex Load History on Fatigue Life, M.S. Rosenfeld, Editor. Philadelphia: American Society for Testing and Materials, ASTM STP 462: p 1-14 (1970).

### Vita

Captain Rodney L. Wilkinson was born on 24 August 1958 in Charleston, West Virginia. He grew up on a small farm in the rural community of Pliny and graduated from Winfield High School in 1976. He then left West Virginia to attend the US Air Force Academy in Colorado, where he graduated in 1980 with a bachelor of science in engineering mechanics. His first active duty assignment was to the Flight Dynamics Laboratory (Air Force Wright Aeronautical Laboratories) at Wright-Patterson AFB, Ohio. After working for three and one-half years as a structural integrity engineer, he was selected in December 1983 to serve as the Laboratory Executive Officer. In May 1984, he entered the Graduate Systems Management program at the Air Force Institute of Technology.

Permanent Address: Route 1, Box 12

Pliny, West Virginia 25158

UNCLASSIFIED

SECURITY CLASSIFICATION OF THIS PAGE

AD-A160146

## REPORT DOCUMENTATION PAGE

1a. REPORT SECURITY CLASSIFICATION <b>UNCLASSIFIED</b>			1b. RESTRICTIVE MARKINGS		
2a. SECURITY CLASSIFICATION AUTHORITY			3. DISTRIBUTION/AVAILABILITY OF REPORT Approved for public release; distribution unlimited.		
2b. DECLASSIFICATION/DOWNGRADING SCHEDULE					
4. PERFORMING ORGANIZATION REPORT NUMBER(S) <b>AFIT/GSM/ENS/85S-32</b>			5. MONITORING ORGANIZATION REPORT NUMBER(S)		
6a. NAME OF PERFORMING ORGANIZATION <b>School of Systems &amp; Logistics</b>		6b. OFFICE SYMBOL (If applicable) <b>AFIT/LSY</b>		7a. NAME OF MONITORING ORGANIZATION	
6c. ADDRESS (City, State and ZIP Code) <b>Air Force Institute of Technology Wright-Patterson AFB, Ohio 45433</b>				7b. ADDRESS (City, State and ZIP Code)	
8a. NAME OF FUNDING/SPONSORING ORGANIZATION <b>Flight Dynamics Laboratory</b>		8b. OFFICE SYMBOL (If applicable) <b>AFWAL/FIBEC</b>		9. PROCUREMENT INSTRUMENT IDENTIFICATION NUMBER	
8c. ADDRESS (City, State and ZIP Code) <b>Wright-Patterson AFB, Ohio 45433</b>				10. SOURCE OF FUNDING NOS.	
				PROGRAM ELEMENT NO.	PROJECT NO.
11. TITLE (Include Security Classification) <b>See Box 19</b>					
12. PERSONAL AUTHOR(S) <b>Rodney L. Wilkinson, B.S., Capt, USAF</b>					
13a. TYPE OF REPORT <b>MS Thesis</b>		13b. TIME COVERED FROM _____ TO _____		14. DATE OF REPORT (Yr., Mo., Day) <b>1985 September</b>	
15. PAGE COUNT <b>144</b>					
16. SUPPLEMENTARY NOTATION					
17. COSATI CODES			18. SUBJECT TERMS (Continue on reverse if necessary and identify by block number)		
FIELD	GROUP	SUB. GR.	Individual Aircraft Tracking    Crack Growth Life Prediction                      Stochastic Fatigue Spectrum Loading                    Fatigue Variability		
01	03				
12	01				
19. ABSTRACT (Continue on reverse if necessary and identify by block number)					
<p>Title: <b>PROBABILISTIC EVALUATION OF INDIVIDUAL AIRCRAFT TRACKING TECHNIQUES</b></p> <p>Thesis Chairman: <b>Joseph W. Coleman, Lieutenant Colonel, USAF</b> Assistant Professor of Operations Research</p> <p style="text-align: right;">Approved for public release: 01/7 APR 1980-1/1. <i>John W. Coleman</i> 11 Sept 85 Head of Operations Research and Development Air Force Institute of Technology Wright-Patterson AFB, Ohio 45433</p>					
20. DISTRIBUTION/AVAILABILITY OF ABSTRACT <b>UNCLASSIFIED/UNLIMITED</b> <input checked="" type="checkbox"/> SAME AS RPT. <input type="checkbox"/> DTIC USERS <input type="checkbox"/>			21. ABSTRACT SECURITY CLASSIFICATION <b>UNCLASSIFIED</b>		
22a. NAME OF RESPONSIBLE INDIVIDUAL <b>Joseph W. Coleman, Lieutenant Colonel, USAF</b>		22b. TELEPHONE NUMBER (Include Area Code) <b>513-255-3871</b>		22c. OFFICE SYMBOL <b>AFHRL/LRA</b>	

A study was conducted in order to demonstrate a technique for comparing the outputs of various individual aircraft tracking (IAT) systems. There were two objectives: (1) to determine the distribution of structural lives that could be expected based on a single IAT scenario, and (2) to evaluate the feasibility of replacing the current universal IAT safety factor with specific statistical calculations that consider the strengths and weaknesses of each IAT system. The ultimate goal of this thesis was to begin the transition of individual aircraft tracking from a deterministic approach to a stochastic one.

A simulation was performed which included twelve aircraft, each flying five different load history variations at three gross weights. Initial structural damage was assumed based on a "reset" flaw size after nondestructive inspection. Structural lives were normally distributed with a mean of approximately 4700 flight hours. The cracks present at the one-half lifetime depot inspection were lognormally distributed. Using these distributions, the probabilities of structural failure were calculated for several inspection intervals. Repeating this process for other IAT scenarios would allow a direct comparison of various IAT systems. Eventually, such a process could lead to individual system safety factors, rather than the current universal safety factor. (Enc. 1)

**END**

**FILMED**

**11-85**

**DTIC**